



**IJOER**  
RESEARCH JOURNAL

# International Journal of Engineering Research & Science

ISSN  
2395-6992

[www.ijoer.com](http://www.ijoer.com)  
[www.adpublications.org](http://www.adpublications.org)

Volume-6! Issue-12! December, 2020 [www.ijoer.com](http://www.ijoer.com) ! [info@ijoer.com](mailto:info@ijoer.com)

## Preface

We would like to present, with great pleasure, the inaugural volume-6, Issue-12, December 2020, of a scholarly journal, *International Journal of Engineering Research & Science*. This journal is part of the AD Publications series *in the field of Engineering, Mathematics, Physics, Chemistry and science Research Development*, and is devoted to the gamut of Engineering and Science issues, from theoretical aspects to application-dependent studies and the validation of emerging technologies.

This journal was envisioned and founded to represent the growing needs of Engineering and Science as an emerging and increasingly vital field, now widely recognized as an integral part of scientific and technical investigations. Its mission is to become a voice of the Engineering and Science community, addressing researchers and practitioners in below areas

Chemical Engineering	
Biomolecular Engineering	Materials Engineering
Molecular Engineering	Process Engineering
Corrosion Engineering	
Civil Engineering	
Environmental Engineering	Geotechnical Engineering
Structural Engineering	Mining Engineering
Transport Engineering	Water resources Engineering
Electrical Engineering	
Power System Engineering	Optical Engineering
Mechanical Engineering	
Acoustical Engineering	Manufacturing Engineering
Optomechanical Engineering	Thermal Engineering
Power plant Engineering	Energy Engineering
Sports Engineering	Vehicle Engineering
Software Engineering	
Computer-aided Engineering	Cryptographic Engineering
Teletraffic Engineering	Web Engineering
System Engineering	
Mathematics	
Arithmetic	Algebra
Number theory	Field theory and polynomials
Analysis	Combinatorics
Geometry and topology	Topology
Probability and Statistics	Computational Science
Physical Science	Operational Research
Physics	
Nuclear and particle physics	Atomic, molecular, and optical physics
Condensed matter physics	Astrophysics
Applied Physics	Modern physics
Philosophy	Core theories

Chemistry	
Analytical chemistry	Biochemistry
Inorganic chemistry	Materials chemistry
Neurochemistry	Nuclear chemistry
Organic chemistry	Physical chemistry
Other Engineering Areas	
Aerospace Engineering	Agricultural Engineering
Applied Engineering	Biomedical Engineering
Biological Engineering	Building services Engineering
Energy Engineering	Railway Engineering
Industrial Engineering	Mechatronics Engineering
Management Engineering	Military Engineering
Petroleum Engineering	Nuclear Engineering
Textile Engineering	Nano Engineering
Algorithm and Computational Complexity	Artificial Intelligence
Electronics & Communication Engineering	Image Processing
Information Retrieval	Low Power VLSI Design
Neural Networks	Plastic Engineering

Each article in this issue provides an example of a concrete industrial application or a case study of the presented methodology to amplify the impact of the contribution. We are very thankful to everybody within that community who supported the idea of creating a new Research with IJOER. We are certain that this issue will be followed by many others, reporting new developments in the Engineering and Science field. This issue would not have been possible without the great support of the Reviewer, Editorial Board members and also with our Advisory Board Members, and we would like to express our sincere thanks to all of them. We would also like to express our gratitude to the editorial staff of AD Publications, who supported us at every stage of the project. It is our hope that this fine collection of articles will be a valuable resource for *IJOER* readers and will stimulate further research into the vibrant area of Engineering and Science Research.



Mukesh Arora  
(Chief Editor)

## **Board Members**

### **Mukesh Arora (Editor-in-Chief)**

BE(Electronics & Communication), M.Tech(Digital Communication), currently serving as Assistant Professor in the Department of ECE.

### **Prof. Dr. Fabricio Moraes de Almeida**

Professor of Doctoral and Master of Regional Development and Environment - Federal University of Rondonia.

### **Dr. Parveen Sharma**

Dr Parveen Sharma is working as an Assistant Professor in the School of Mechanical Engineering at Lovely Professional University, Phagwara, Punjab.

### **Prof.S.Balamurugan**

Department of Information Technology, Kalaignar Karunanidhi Institute of Technology, Coimbatore, Tamilnadu, India.

### **Dr. Omar Abed Elkareem Abu Arqub**

Department of Mathematics, Faculty of Science, Al Balqa Applied University, Salt Campus, Salt, Jordan, He received PhD and Msc. in Applied Mathematics, The University of Jordan, Jordan.

### **Dr. AKPOJARO Jackson**

Associate Professor/HOD, Department of Mathematical and Physical Sciences, Samuel Adegboyega University, Ogwa, Edo State.

### **Dr. Ajoy Chakraborty**

Ph.D.(IIT Kharagpur) working as Professor in the department of Electronics & Electrical Communication Engineering in IIT Kharagpur since 1977.

### **Dr. Ukar W.Soelistijo**

Ph D , Mineral and Energy Resource Economics, West Virginia State University, USA, 1984, Retired from the post of Senior Researcher, Mineral and Coal Technology R&D Center, Agency for Energy and Mineral Research, Ministry of Energy and Mineral Resources, Indonesia.

### **Dr. Samy Khalaf Allah Ibrahim**

PhD of Irrigation &Hydraulics Engineering, 01/2012 under the title of: "Groundwater Management Under Different Development Plans In Farafra Oasis, Western Desert, Egypt".

### **Dr. Ahmet ÇİFCİ**

Ph.D. in Electrical Engineering, Currently Serving as Head of Department, Burdur Mehmet Akif Ersoy University, Faculty of Engineering and Architecture, Department of Electrical Engineering (2015-...)

### **Dr. Mohamed Abdel Fatah Ashabrawy Moustafa**

Ph.D. in Computer Science - Faculty of Science - Suez Canal University University, 2010, Egypt.

Assistant Professor Computer Science, Prince Sattam bin AbdulAziz University ALkharj, KSA.

### **Dr. Heba Mahmoud Mohamed Afify**

Ph.D degree of philosophy in Biomedical Engineering, Cairo University, Egypt worked as Assistant Professor at MTI University.

### **Dr. Aurora Angela Pisano**

Ph.D. in Civil Engineering, Currently Serving as Associate Professor of Solid and Structural Mechanics (scientific discipline area nationally denoted as ICAR/08—"Scienza delle Costruzioni"), University Mediterranea of Reggio Calabria, Italy.

### **Dr. Faizullah Mahar**

Associate Professor in Department of Electrical Engineering, Balochistan University Engineering & Technology Khuzdar. He is PhD (Electronic Engineering) from IQRA University, Defense View, Karachi, Pakistan.

### **Dr. S. Kannadhasan**

Ph.D (Smart Antennas), M.E (Communication Systems), M.B.A (Human Resources).

### **Dr. Christo Ananth**

Ph.D. Co-operative Networks, M.E. Applied Electronics, B.E Electronics & Communication Engineering Working as Associate Professor, Lecturer and Faculty Advisor/ Department of Electronics & Communication Engineering in Francis Xavier Engineering College, Tirunelveli.

### **Dr. S.R.Boselin Prabhu**

Ph.D, Wireless Sensor Networks, M.E. Network Engineering, Excellent Professional Achievement Award Winner from Society of Professional Engineers Biography Included in Marquis Who's Who in the World (Academic Year 2015 and 2016). Currently Serving as Assistant Professor in the department of ECE in SVS College of Engineering, Coimbatore.

### **Dr. Maheshwar Shrestha**

Postdoctoral Research Fellow in DEPT. OF ELE ENGG & COMP SCI, SDSU, Brookings, SD  
Ph.D, M.Sc. in Electrical Engineering from SOUTH DAKOTA STATE UNIVERSITY, Brookings, SD.

### **Zairi Ismael Rizman**

Senior Lecturer, Faculty of Electrical Engineering, Universiti Teknologi MARA (UiTM) (Terengganu) Malaysia  
Master (Science) in Microelectronics (2005), Universiti Kebangsaan Malaysia (UKM), Malaysia. Bachelor (Hons.) and Diploma in Electrical Engineering (Communication) (2002), UiTM Shah Alam, Malaysia

### **Dr. D. Amaranatha Reddy**

Ph.D.(Postdoctoral Fellow,Pusan National University, South Korea), M.Sc., B.Sc. : Physics.

## **Dr. Dibya Prakash Rai**

Post Doctoral Fellow (PDF), M.Sc.,B.Sc., Working as Assistant Professor in Department of Physics in Pachhunga University College, Mizoram, India.

## **Dr. Pankaj Kumar Pal**

Ph.D R/S, ECE Deptt., IIT-Roorkee.

## **Dr. P. Thangam**

BE(Computer Hardware & Software), ME(CSE), PhD in Information & Communication Engineering, currently serving as Associate Professor in the Department of Computer Science and Engineering of Coimbatore Institute of Engineering and Technology.

## **Dr. Pradeep K. Sharma**

PhD., M.Phil, M.Sc, B.Sc, in Physics, MBA in System Management, Presently working as Provost and Associate Professor & Head of Department for Physics in University of Engineering & Management, Jaipur.

## **Dr. R. Devi Priya**

Ph.D (CSE),Anna University Chennai in 2013, M.E, B.E (CSE) from Kongu Engineering College, currently working in the Department of Computer Science and Engineering in Kongu Engineering College, Tamil Nadu, India.

## **Dr. Sandeep**

Post-doctoral fellow, Principal Investigator, Young Scientist Scheme Project (DST-SERB), Department of Physics, Mizoram University, Aizawl Mizoram, India- 796001.

## **Mr. Abilash**

MTech in VLSI, BTech in Electronics & Telecommunication engineering through A.M.I.E.T.E from Central Electronics Engineering Research Institute (C.E.E.R.I) Pilani, Industrial Electronics from ATI-EPI Hyderabad, IEEE course in Mechatronics, CSHAM from Birla Institute Of Professional Studies.

## **Mr. Varun Shukla**









M.Tech in ECE from RGPV (Awarded with silver Medal By President of India), Assistant Professor, Dept. of ECE, PSIT, Kanpur.

## **Mr. Shrikant Harle**

Presently working as a Assistant Professor in Civil Engineering field of Prof. Ram Meghe College of Engineering and Management, Amravati. He was Senior Design Engineer (Larsen & Toubro Limited, India).

# Table of Contents

Volume-6, Issue-12, December 2020

S.No	Title	Page No.
1	<b>Detection of Xylene (C<sub>8</sub>H<sub>10</sub>) by Pd-gate MOS Sensor</b> <b>Authors:</b> J.K. Srivastava, K.K. Verma  DOI: <a href="https://dx.doi.org/10.5281/zenodo.4400119">https://dx.doi.org/10.5281/zenodo.4400119</a>  <b>DIN Digital Identification Number:</b> IJOER-DEC-2020-1	01-06
2	<b>Trimaran Fishing Vessel Development: A Review of Vessel Power, Safety and Comfort Needs</b> <b>Authors:</b> Richard Benny Luhulima  DOI: <a href="https://dx.doi.org/10.5281/zenodo.4400121">https://dx.doi.org/10.5281/zenodo.4400121</a>  <b>DIN Digital Identification Number:</b> IJOER-DEC-2020-9	07-13
3	<b>Effect of Citric Acid on Thickeners Used in Products for People Suffering Oropharyngeal Dysphagia</b> <b>Authors:</b> Josep García Raurich, Anna Mas Herrador, Queralt Pérez Ruiz  DOI: <a href="https://dx.doi.org/10.5281/zenodo.4400125">https://dx.doi.org/10.5281/zenodo.4400125</a>  <b>DIN Digital Identification Number:</b> IJOER-DEC-2020-13	14-24
4	<b>Impact of France Nuclear Tests on typhoons and Earthquakes in November 1990</b> <b>Authors:</b> Vladimir Kostin, Gennady Belyaev, Olga Ovcharenko, Elena Trushkina  DOI: <a href="https://dx.doi.org/10.5281/zenodo.4400127">https://dx.doi.org/10.5281/zenodo.4400127</a>  <b>DIN Digital Identification Number:</b> IJOER-DEC-2020-14	25-31



# Detection of Xylene ( $C_8H_{10}$ ) by Pd-gate MOS Sensor

J. K. Srivastava<sup>1\*</sup>, K. K. Verma<sup>2</sup>

Dr. Ram Manohar Lohia, Awadh University, Department of Physics & Electronics, Ayodhya, India

**Abstract**— A sensor based on Pd/SiO<sub>2</sub>/Si MOS capacitor was fabricated on p type <100> (1-6 ΩCm) Si with thermal oxide layer of thickness about 200 Å. The sensor showed sensitivity to Xylene ( $C_8H_{10}$ ) vapour and was characterized at Xylene concentrations ranging from (500ppm-16,000ppm) at different operating temperatures (room temperature, 70°C and 120°C), in air. It was found that sensitivity of the sensor was maximum at an operating temperature of 70°C.

**Keywords**— MOS (metal-oxide- semiconductor) structure, gas sensor, Palladium (Pd), sensitivity, C-V and G-V characteristics.

## I. INTRODUCTION

The sensors capable of detecting the toxic as well as explosive gases such as Xylene which is known to be having very serious effects on the respiratory systems are need to be developed. The promise of small integrated sensors with high sensitivity has motivated the numerous researchers [1-4] to develop and study the gas sensors based on Pd gate MOS structure. These sensors have been found to be sensitive for hydrogen and the detection mechanism could be attributed to change in metal work function on exposure to hydrogen. [5,6]. The model for mechanism of hydrogen sensitivity of Pd MOS device has been proposed by Lundstrom et al. [7]. Exposure of hydrogen gas on the sensor causes the hydrogen molecule to dissociate into atomic hydrogen on Pd surface, and then these atoms diffuse through the Pd film and get adsorbed at Pd/insulator interface. The adsorbed and dissolved hydrogen atoms give rise to the formation of dipole layer at the Pd/insulator interface and work function of the Pd is decreased which can be measured in terms of change in flat band voltage of the MOS capacitor [7]. It is possible to detect the hydrocarbons or other hydrogen containing gases by these sensors provided they can be dehydrogenated on the Pd surface, so that hydrogen atoms can diffuse and are adsorbed on Pd/insulator interface and give rise to change in the flat band voltage of the device. This paper presents the result of, analysis of C-V and G-V responses of Pd gate MOS capacitors, exposed to various Concentration (500 ppm – 1.6 %) of Xylene vapors, in air at several temperatures. It is found that Pd gate becomes more sensitive to Xylene, in air at operating temperature 70°C.

## II. EXPERIMENTAL

The SiO<sub>2</sub> based Pd- gate MOS structure was fabricated on a p-type <100>, 3" Silicon substrate and its structure is shown in fig. 1.

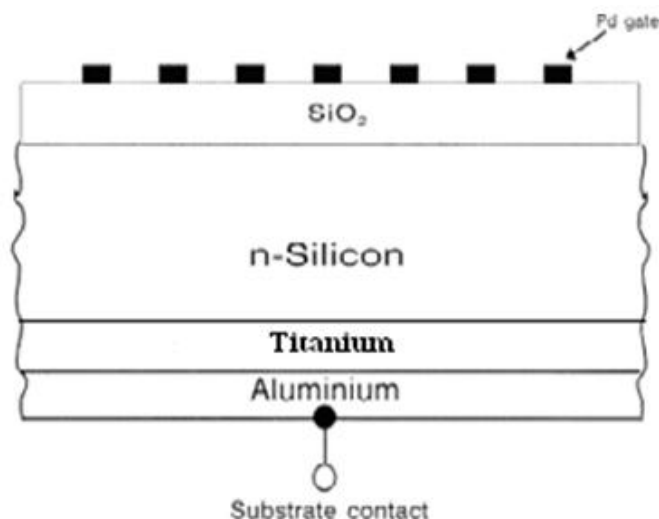


**FIGURE 1: Cross sectional view of the fabricated sensor**

For fabrication of MOS capacitor, the wafer was thoroughly cleaned using standard technological cleaning procedures used in silicon technology. SiO<sub>2</sub> layer was grown by dry thermal oxidation of silicon wafer in the oxidation furnace (at 900°C for 12 min.). Subsequently, photolithography technique was used for retaining front side oxide and removing back side oxide.



Palladium was deposited on the front face of the wafer by vacuum evaporation method, using standard mask having holes of 1mm. diameter for gate. The ohmic contact to the back side of Si substrate was made by evaporating Al metal. Annealing was done at  $450^{\circ}\text{C}$  in nitrogen ambient for 7 minutes, for achieving a proper front and back contacts. The experimental set-up used to study the C-V and G-V response of the fabricated device with exposure to xyelene is shown in fig 2. C-V and G-V characteristics of fabricated MOS sensor was studied at different concentration of dyelines with the help of C-V analyzer, (model 590 KEITHLEY Instruments, USA) and Precision LCR meter HP-4284A (having frequency range of 20Hz-1MHz). Both the Instruments were interfaced to a PC. ICS (Interactive characterization software) software was used to obtain the accurate information from the instruments and stored in computer.

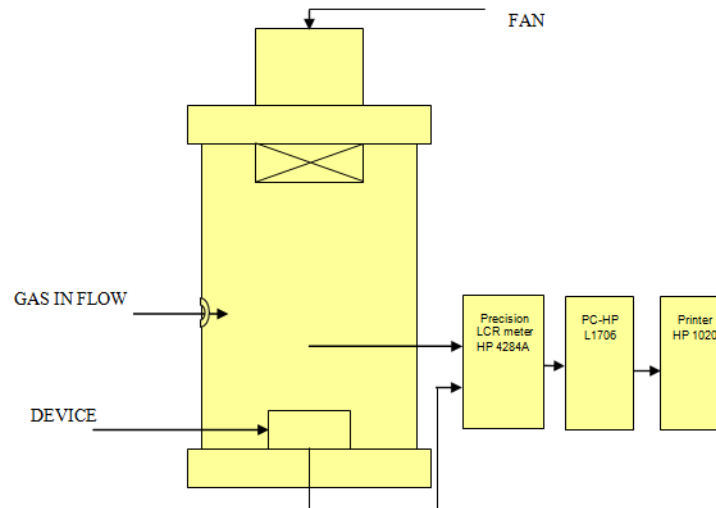


**FIGURE 2: Block diagram for experimental set-up**

### III. RESULTS

#### 3.1 C-V measurements

The variation of capacitance with gate voltage for fabricated Pd gate MOS capacitor, in air, as well as upon exposure to different concentrations (500 ppm- 16,000 ppm) of xyelene at 100 kHz frequency was recorded at different operating temperatures( room temperature,  $70^{\circ}\text{C}$  and  $120^{\circ}\text{C}$ ) and the obtained results are shown in fig (3-5).

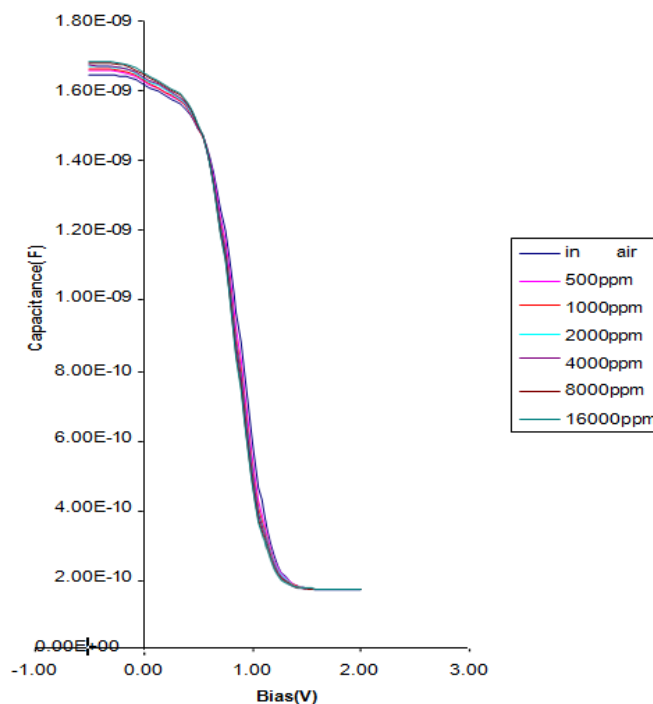


**FIGURE 3: C-V response of Pd gate MOS sensor at room temperature**

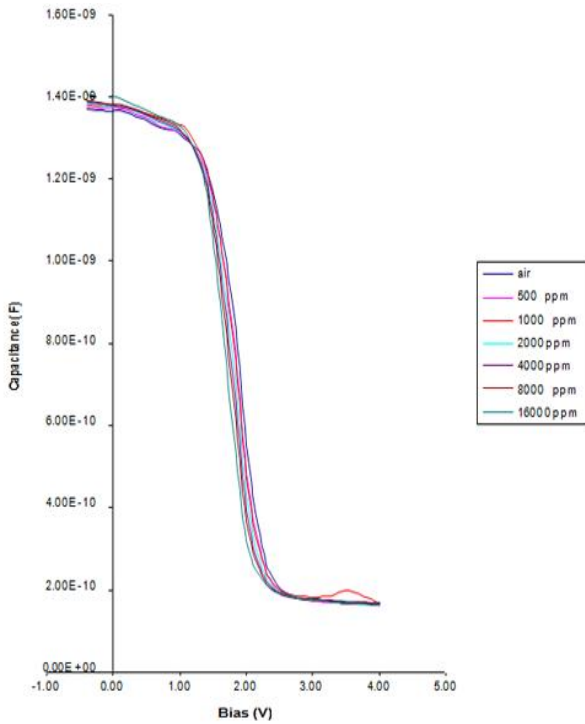


**FIGURE 4: C-V response of Pd gate MOS sensor at 70°C**

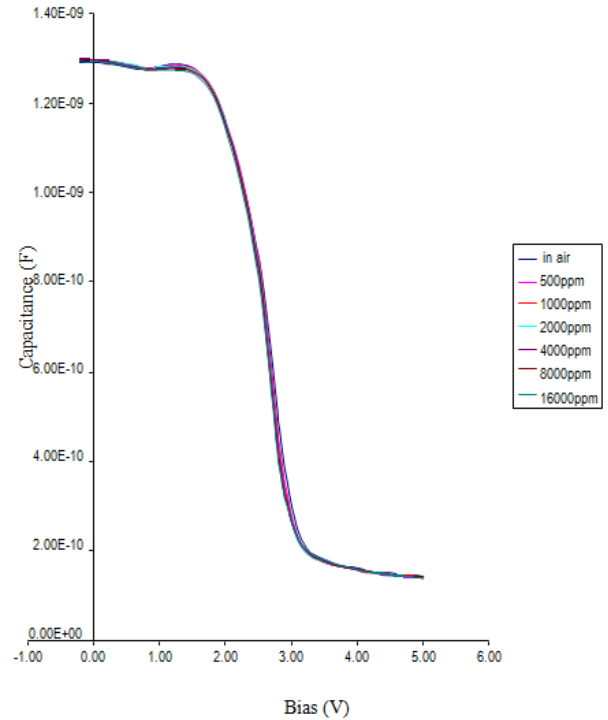


**FIGURE 5: C-V response of Pd gate MOS sensor at 120°C**

It can be observed that exposure of the sensor to higher Xylene concentration causes a shift of whole C-V curve to more negative side of the voltage axis and this shift is most prominent when device is heated at temperature at of 70°C. It is also inferred from these figures that as the concentration of Xylene increases capacitance decreases and maximum change in the capacitance always occurs at the same bias voltage for all concentration levels at a given operating temperature and sensitivity increases with the higher concentration.

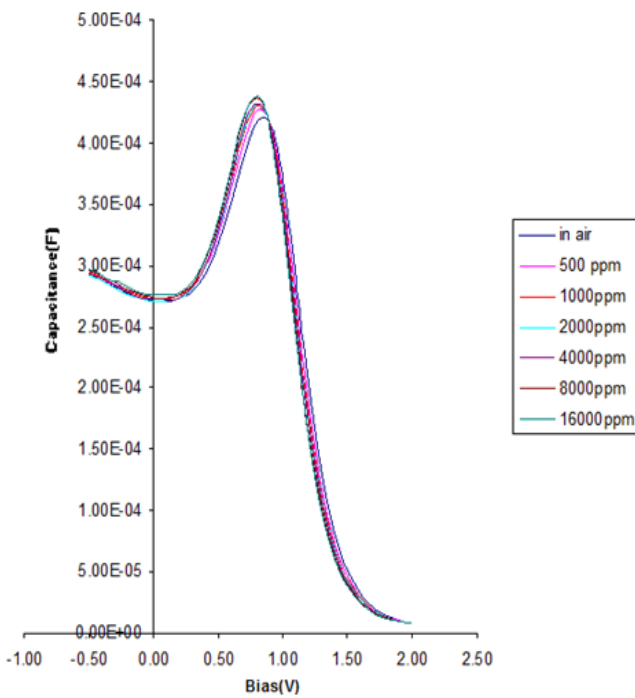


**FIGURE 6: G-V response of Pd gate MOS sensor at room temperature**

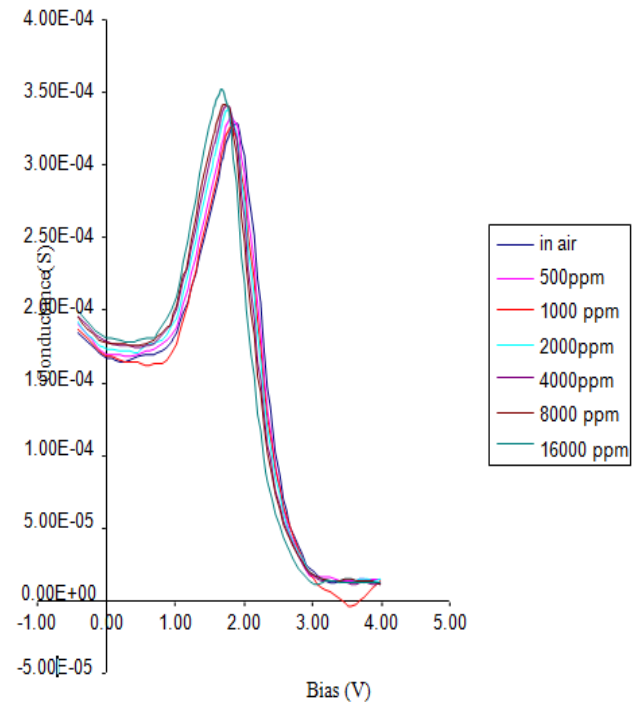


**FIGURE 7: G-V response of Pd gate MOS sensor at 70°C**

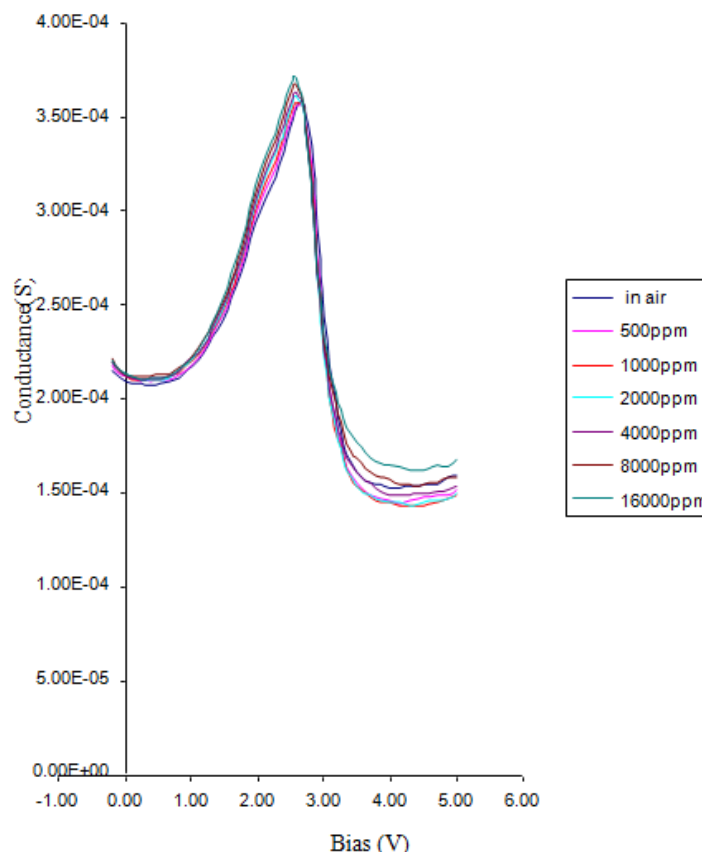


**FIGURE 8: G-V Response of Pd gate MOS sensor at 120<sup>0</sup> C**

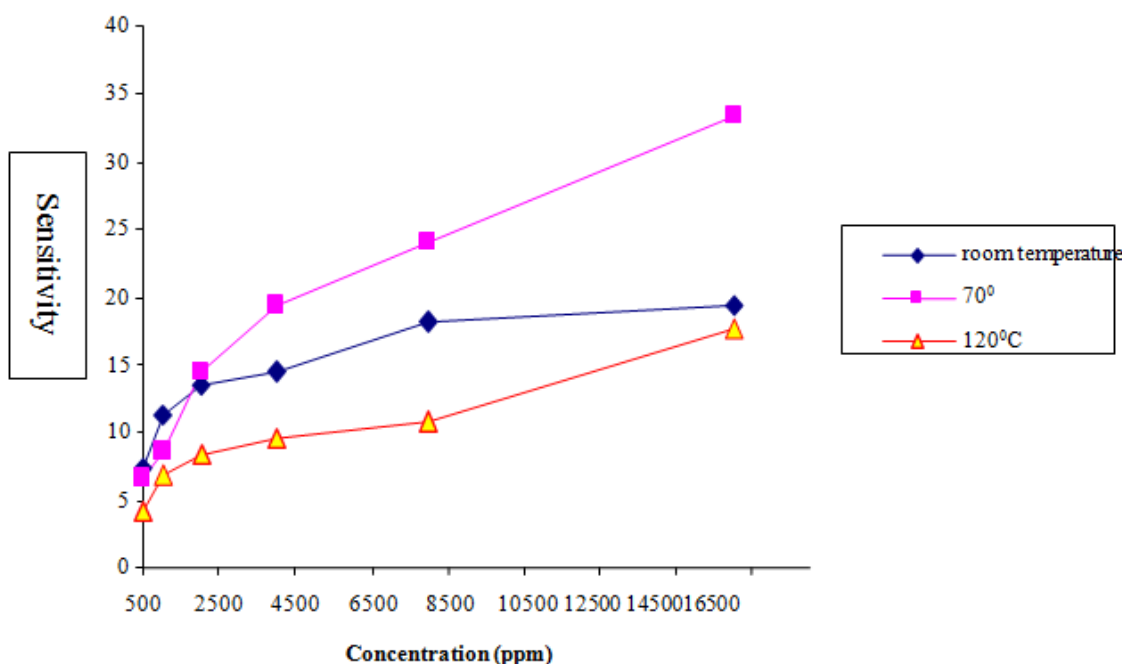


**FIGURE 9: Variation of sensitivity with concentration at different operating temp. on exposure to Xylene**

The variation of sensitivity with concentration at different operating temperatures is shown in fig. 9. The maximum sensitivity (33. 3%) is found at operating temperature 70°C, where as for room temperature measurements the sensitivity reduces to 21. 6% at bias voltage of 0. 9 volts. The figures also reveal that flat band voltage of the sensor decreases by 200 mV at room temperature where as this change in  $V_{fb}$  becomes 380 mV at an operating temperature of 70°C, which again shows that sensitivity of the sensor is much improved at this operating temperature.

### 3.2 G-V measurements

Figures (6-8) show the variation of conductance with bias voltage for the fabricated sensor, with varying concentration of xyelene, at different operating temperatures. These figures show that as the concentration of xyelene increases the peak magnitude of conductance increases and becomes saturated at particular concentration (1.6 %). The conductance peak position also shifts towards left with Xyelene concentration. This shift is maximum (12.5%) at an operating temperature 70°C and reduces to 8.42% at room temperature. Hence sensitivity of the sensor is again found to be highest at 70°C if it is defined as

$$S(\%) = \frac{\Delta G}{G} \times 100$$

Where

G- Initial conductance peak position in air

$\Delta G$ - shift in conductance peak position at certain xyelene concentration

## IV. DISCUSSION

From the previous works [1-4] it is well known that MOS capacitor with Pd gate show a lateral shift in the flat band voltage of the device on exposure to hydrogen gas. The hydrogen molecules are adsorbed and dissociated at the Pd surface. Some of the adsorbed atoms move at the Pd/ insulator interface, which give rise to change in electronic work function of the Pd surface due to their dipole moments. And therefore affects the flat band voltage of the device. When hydrogen gas is removed, the flat band voltage reduces to its original value [3].

In present work, the sensitivity of the sensor towards Xyelene vapors is probably due to catalytic dissociation of Xyelene molecules into hydrogen and carbon atoms. It can be believed that only hydrogen atoms have the accessibility to diffuse through the Pd layer to Pd/ SiO<sub>2</sub> interface, where they give rise to formation of dipole layer and change in flat band voltage of the device [3]. Dissociation of hydrocarbons on metals like Pd has been already reported by various researchers [8, 9]. The variational behavior of capacitance and conductance with temperature may be due to thermal generation of charge carriers, which increases with increase in temperature. Also the significant response of minority carriers at elevated temperature and contribution of induced surface traps to generation-recombination at higher temperature may be responsible for variation in C-V and G-V response of fabricated sensor.

At higher temperature, hot Pd surface in air, will act as dehydrogenation catalyst for Xyelene and will accelerate the dissociation process, resulting in greater number of available hydrogen atoms (as compared to room temperature) which are adsorbed at the metal surface to diffuse into the oxide layer and give better response. Hence sensitivity should increase with temperature as expected. However in present study, sensitivity is becoming maximum at 70° C and decreasing beyond this temperature. It can be accounted for by high concentration of surface states in the oxide layer and at “insulator/semiconductor” interface. Probably, the negatively charged oxygen ions which are adsorbed at the metal surface combine with H<sup>+</sup> to form OH<sup>-</sup> which diffuses into the oxide layer to form an extra charge layer and ultimately modulating the surface states. At higher temperature, this process should increase but it seems that at 70° C the coverage of OH<sup>-</sup> is saturated at the metal surface and beyond this temperature surface states modulation do not have a dominant effect on the sensitivity and now only the minority and thermally generated charge carriers have predominant contribution which results in fall in the sensitivity beyond 70° C.

The measurements also show that peak conductance value increases with Xyelene concentrations which can be attributed to the increase in interface charge density as reported by the numerous researchers (10-12) on exposure of hydrogen. In the present case also xyelene ultimately dissociates into hydrogen which increases the interface charges. The increase in peak conductance value is higher (8.64%) at operating temperature of 70°C as compared to the room temperature (3.34%) can again be explained by considering the improved dehydrogenation at higher temperature and better availability of the hydrogen atoms at Pd/ SiO<sub>2</sub> interface.

## V. CONCLUSION

It is concluded that Pd-gate MOS capacitor is a promising sensor for xyelene sensing. The highest sensitivity (33.3% in terms of capacitance measurement and 8.42% in terms of conductance) is found when operating temperature is 70°C. The

change in the flat band voltage of the sensor is also found to be greater (380 mV) at 70°C as compared to operation at room temperature (200mV) when Xylene concentration is varied from 500 ppm to 16,000 ppm.

### REFERENCES

- [1] Claes Nylander, Marten Armgrath and Christer Svensson, Hydrogen induced drift in Palladium gate metal-oxide-semiconductor structures, *J. Appl. Physics*, 56(4),1984,(1177-1186)
- [2] P. F. Ruths, S. Ashok, S. J. Fonash, J. M. Ruths, A study of MIS Schottky-barrier diode detector. *IEEE Trans. Electron devices* ED28 (1981) 1003-1009
- [3] I. Lundstrom, S. Shivaraman, C. Svensson and L. Lundkvist, A hydrogen sensitive MOS field effective transistor, *Appl. Phys. Lett.* 26 (1975), pp. 55-57.
- [4] I. Lundstrom, Hydrogen sensitive MOS structure: Part 1. Principles and applications. *Sensor and Actuators* (1981) 403-426.
- [5] L. G. Petersson, H. M. Dannetun, J. Fogelberg and I. Lundstrom, Hydrogen adsorption states at the external and internal palladium-silicon dioxide-silicon structure, *J. Appl. Physics* 58(1985), 404-413.
- [6] I. Lundstrom and L. G. Petersson, chemical sensors with catalytic metal gate, *J. Vac. Sci. Technol. A*14 (1996), 1539-1545,
- [7] M. S. Shivaraman, I. Lundstrom, C. Svensson, H. Hammarsten, Hydrogen sensitivity of palladium-thin-oxide-silicon Schottky barriers. *Electron. Lett.* (1976) 484-485.
- [8] D. Al-Mawlawi and J. M. Saleh, Interactions of alcohols with evaporated metal films, *J. Chem. Soc., Faraday Trans. 1*, vol. 77,(1981) 2965-2976( part 1), 2977-2988 (part 2).
- [9] H. Jacobs, W. Mokwa, D. Kohl, and G. Heiland, Decomposition of ethanol on a ZnO supported Pd catalyst, *Surface Sci.*, vol. 126,(1983) 368-373.
- [10] H. Kobayashi, H. Iwadate, Y. Kogestu, Y. Nakato, Mechanism of the formation of hydrogen-induced interface states for Pt/SiO<sub>2</sub>/silicon MOS tunneling diodes. *J. Appl. Physics* 78(1995) 6554- 6561.
- [11] Mark A. Formso and G. Jordan Maclay, The effect of hydrogen and Carbon Monoxide on the Interface state density in MOS gas sensors with ultra thin Palladium Gates, *Sensors and actuators B*, 2 (1990) 11-22.
- [12] D. Dwivedi, R. Dwivedi, S. K. Srivastava, "Sensing properties of palladium-gate MOS (Pd- MOS) hydrogen sensor-based on plasma grown silicon dioxide" *Sensors and actuators B*71(2000) 161-168.

# Trimaran Fishing Vessel Development: A Review of Vessel Power, Safety and Comfort Needs

Richard Benny Luhulima

<sup>1</sup>Department of Naval Architecture, Pattimura University, Indonesia

**Abstract**— In general, fishing fleets operating in Maluku waters and managed by local entrepreneurs consist of mono hull fishing vessels (such as purse seines, etc.) and trimaran in chart form. These two types of fishing fleets have been known to the people of Maluku for a long time. However, these two types each have their advantages and limitations, for example, mono hull fishing boats have limited deck space and poor transverse stability, especially in bumpy sea conditions in extreme weather. While the trimaran type has better deck space and transverse stability than a mono hull ship, but because it is still in chart form, it has limited space. The shortcomings that exist in these two types of fishing fleets are coupled with the expertise or experience of fishermen which has minimal impact on the decrease in the catch and what is worse can be fatal to accidents and the sinking of ship arma. To increase the catch of fisheries, it is necessary to have a means and a reliable fishing fleet. This study aims to examine the development of trimaran fishing vessels in terms of the study of energy needs, safety and comfort for the captain and crew during fishing operations. The initial stage of this research begins with data analysis and the principal size of mono hull fishing vessels operating in Maluku waters, from this data the hull form of a trimaran vessel is designed with an area similar to or close to the area of a monohull fishing vessel operating in Maluku waters using maxsurf, then analyzed the calculation of obstacles. ship and stability to assess the energy needs and safety and comfort of the ship during fishing operations. This research is focused on analyzing the energy requirements, safety and comfort of the trimaran fishing vessel. The final result of this research is expected to be used as an alternative fishing boat to increase the fish catch of fishermen which will have an impact on the income and welfare of fishermen.

**Keywords**— Trimaran Fishing Vessel, Resistance, Power, Safety, Comfort.

## I. INTRODUCTION

As a province where 92% of its total area is water, the marine and fisheries sector in Maluku Province is the main source of economic growth in the region. Capture fisheries potential in Maluku is recorded at 1.72 million per year. This has prompted the Indonesian government to designate Maluku as the “National Fish Barn.” In a global context, Maluku is an important part of the world's marine biodiversity, considering that this province has 76% of the world's coral species and 37% of the world's coral fish species.

Overfishing is one of the main threats to Maluku's fishery sector which includes the exploitation of shrimp and big-eye tuna, snapper, grouper, flying fish and albakora tuna. The lack of data availability, for example data related to small pelagic fish and large pelagic fish as well as migratory species as well as information on the value and status of coral reefs, seagrass beds and estuary (estuary) ecosystems in Maluku Province is another challenge in fisheries management efforts in Maluku Province. Management of marine conservation areas that are not yet optimal adds to the long list of threats to Maluku's fishery sector. The development of coastal areas that are not environmentally friendly as well as the pollution resulting from the development of public waters needs to be managed through good water zoning planning. Law enforcement efforts are needed to tackle the rampant illegal, unregulated and unreported fishing practices (Illegal, Unregulated, and Unreported / IUU Fishing), shark fishing, destructive fishing practices, wildlife crime, and the lack of capacity of relevant stakeholders.

Fishermen need to have a good boat to be able to catch fish optimally. Fishing boats operating in Maluku waters often experience accidents at sea during fishing operations caused by extreme weather factors, overloading and human error. One way to improve the stability of fishing boats is by changing the shape of the monohull hull to a trimaran. This is because the form of monohull ships that are often found in Maluku waters has several shortcomings in relation to ship stability, as well as limited loading space. The advantages of the trimaran are that it has better stability, longer cruising range, and has smaller ship resistance and friction compared to the monohull hull. Therefore, as an effort to minimize ship accidents, it can be done by implementing the use of the trimaran ship type as an alternative in the procurement and addition of fishing vessels in Maluku. Trimaran ship is a development of a ship model with a multi hull system. Trimaran ships have several advantages compared to monohull ships, for example, on the size of the ship with the same width, the trimaran ship's friction resistance

is smaller, so that it has the thrust with the same speed is greater. The deck area of a trimaran ship is wider than a ship with a monohull hull type. Submerged volume and relatively smaller wet area, better stability because it has multiple hulls.

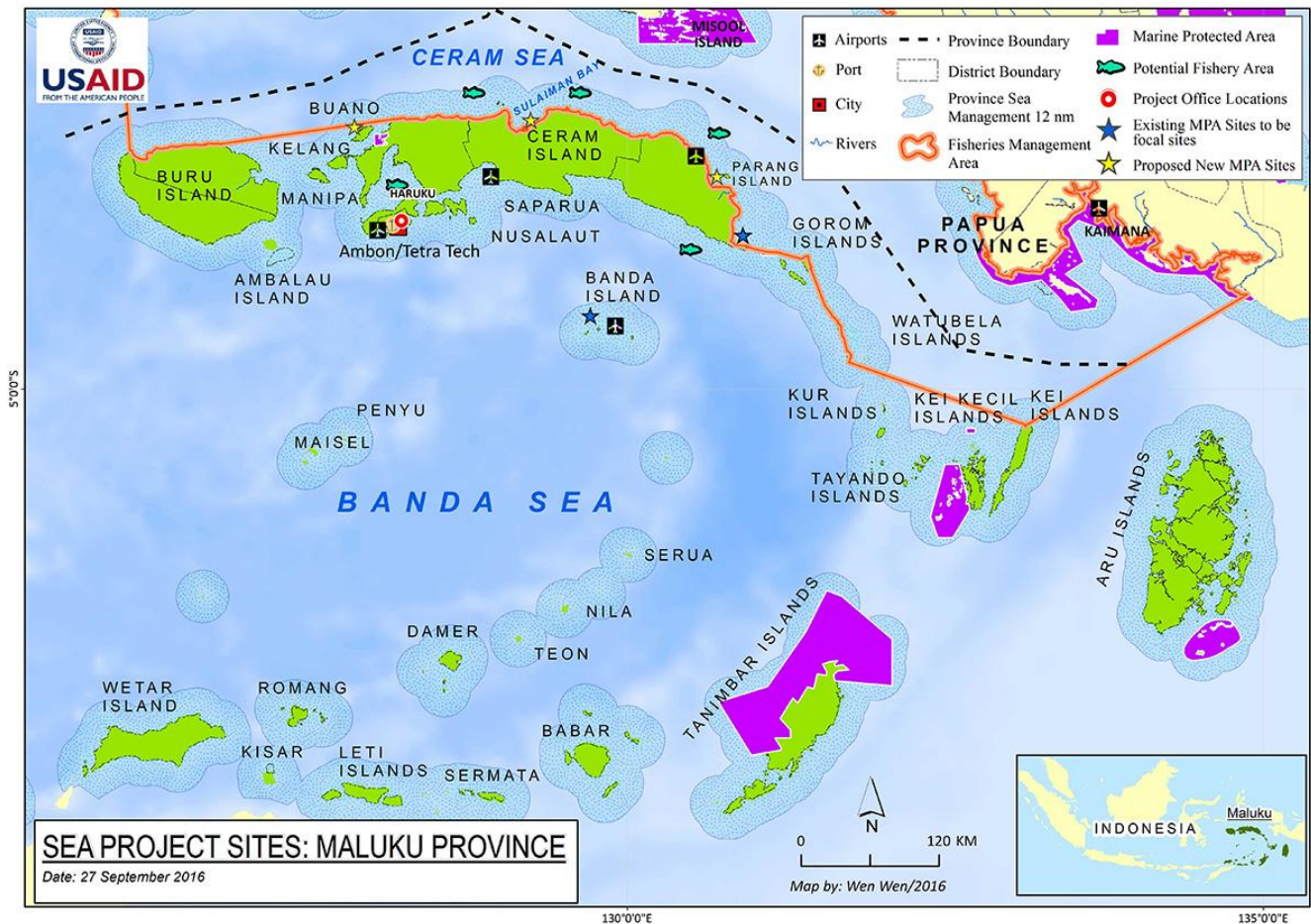


**FIGURE 1: Maluku Province**

The utilization of the installed production capacity of the shipyard industry is now in the range of 50%-60% and to reach a utilization rate of 80% still takes a long time. If the government shows its side, domestic production capacity will increase. Currently, the capacity of building new ships in Indonesia is around 900,000 deadweight tonnage (DWT) ships per year. Meanwhile, the capacity for docking repairs throughout the year is 12 million DWT.

So far, the project for the fisheries sector tends to be small and there is no significant growth. For national needs, Iperindo also admits that it does not know how much fishing vessels need to explore the archipelago at this time. If you trace the projection in 2025, IPERINDO hopes that the shipping industry in the country will be able to build and repair ships with a capacity of 300,000 DWT.

The development of Trimaran fishing vessels has never been carried out by domestic or foreign agencies. Selection of Hull Trimaran is very important because it has a large deck surface and also has good stability. The large deck surface allows crew members to move freely. The Trimaran Fishing Ship is one form of UNPATTI's Leading Strategic Plan to become a national scientific and technological reference center in the field of Shipping and Fisheries.

The purpose of this study was to obtain the shape of the trimaran fishing boat hull. This research is focused on the study of the development of trimaran fishing vessels in terms of energy requirements, safety and comfort of ships during fishing operations. The problems formulated are: Analysis of the development of trimaran fishing vessels in terms of the aspects of energy needs, safety and comfort of the captain and crew. The overall objective of this research is to minimize fishing boat accidents during operation at fishing ground and reduce the Power

From the study conducted can be obtained an effective and power-efficient trimaran fish vessel model. The results of the technology are expected to be well utilized to improve optimal catches and meet environmental safety criteria and obtain abundant catches.



## II. METHOD

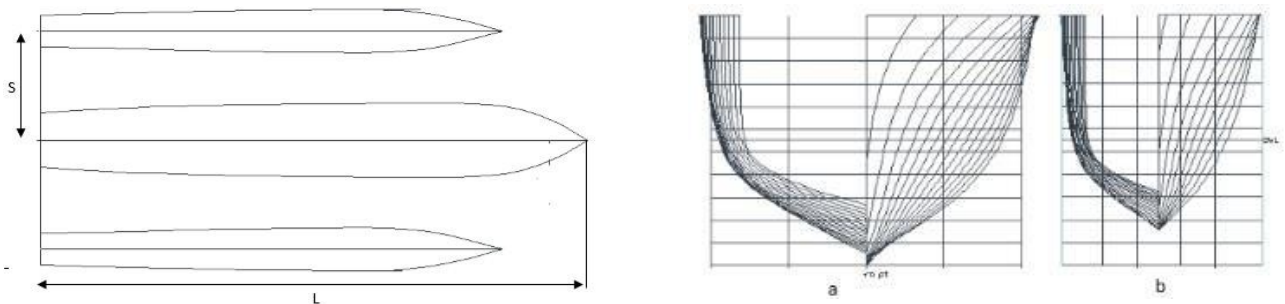


**FIGURE 2: Trimaran Configuration,  $S/L=0.2$**

In the simulation, the amount of resistance components that act on the trimaran hull will be known. Simulation of free-surface modeling (on water and air media) is used to calculate the total resistance on the hull. The wall for the fluid domain in free slip conditions, namely the shear stress on the wall is zero and the velocity near the wall does not experience a slowdown due to the effect of wall friction. In this simulation, the model is created in a no-slip condition (i.e. friction occurs on the model surface). Meanwhile, to calculate the viscous resistance, the hull is immersed (in the water medium) until it is full of water by assuming the top boundary condition is a solid wall and free slip. Then the wave resistance can be calculated from the difference in the value of total resistance and viscous resistance.

The CFD program consists of 4 main elements:

1. ICEM, which is a geometry and meshing design.
2. CFX-pre, is the boundary condition and specific parameter.
3. Solver is an iterative process.
4. CFX-post is a process of analysis.

In the validation process, there are several important parameters that are considered, namely grid (mesh), convergence, and data results experiment.

### 2.1 Convergence

At this stage, the iteration process of calculations will always be controlled by a controlling equation. If the calculation result does not match the specified error rate, the computation will continue. The following are some RMS charts that show the convergence of the iteration process, as shown in Fig 3.

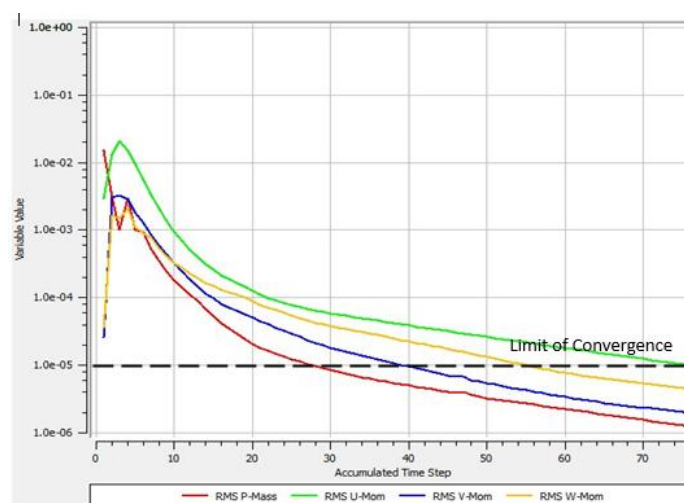


**FIGURE 3: Convergence**

The root-mean square (RMS) criterion used to check the convergence of the free surface simulation is the residual target value (variable value) reaching  $10^{-5}$ . The target criteria (variable value) are widely applied in computational engineering, as recommended in the ANSYS ICEM manual (2007) and Dinham et al (2008).

## 2.2 Grid Independence

The large number of cells or grids used in the calculation will determine the accuracy of the results obtained because the number of cells affects the change in geometric shape during result processing. Figure 4 shows the initial computational domain. The boundary at the front of the hull is up to 1.5 times the length of the hull model, at the back the hull is 4 times the length of the hull. Then sideways are 1.5 times the length of the model and the distance is above 2.5 times the length of the model and under 2 times the length of the hull model. This distance is sufficient to avoid the blockage effect (Utama, 1999; Ahmed and Soares, 2009). The computation for the mesh used (multiphase flow calculations) consisted of 1,582,580 mesh elements.

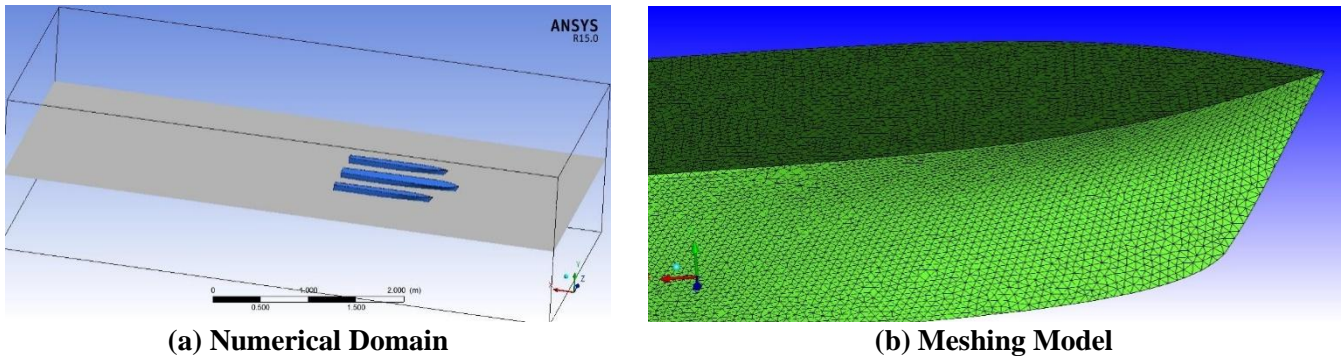


**FIGURE 4: Numerical Model Trimaran**

The quality or number of mesh grids is fundamental to convergence and accuracy of CFD simulation / computation. Grid quality and value are discussed in detail by Thompson et al (1999) and Deng et al (2010). The number of mesh elements, 1582,580 for the trimaran hull is quite optimal and accurate, where the number of elements used in the computation shows that it is grid independence as shown in Figure 4. Resistance values for the number of mesh elements (grid) 1,582,580 and 2,875,830 are constant and the same. So it can be said that the selected 1,582,580 mesh numbers in CFD computation have met a fairly good level of accuracy.

## III. RESULT AND DISCUSSION

### 3.1 Resistance and Power

The trimaran drag component coefficient is symmetrical in the transverse hull distance configuration ( $S/L$ ). For the hull trimaran configuration  $S/L = 0.2$ , presented sequentially in Figure which shows that the viscous resistance is greater (dominant) than the wave resistance at  $Fr < 0.27$ . This is because the hull distance is close enough so that the fluid between the hulls hitting the ship's hull will be reflected to other hulls that are in deep flow. The magnitude of the difference in the viscous coefficient of the ship is shown in Table 1.

The viscous resistance coefficient is very dominant at  $Fr < 0.22$  then at  $S/L > 0.22$  The wave resistance coefficient starts to increase, but the viscous resistance coefficient is more dominant at  $S/L < 0.27$ . This is shown in table 1. Figures 5 show that viscous interference is more dominant than resistance interference.

**TABLE 1  
RESISTANCE COEFFICIENT TRIMARAN VESSEL**

Fr	Coefficient Total ( $C_T$ )	Coefficient Vicous( $C_V$ )	Coefficient Wave ( $C_W$ )
	$(10^{-3})$		
0.15	4.491	4.201	0.29
0.17	4.848	4.11	0.738
0.19	5.258	4.008	1.251
0.21	5.965	3.908	2.057
0.23	6.295	3.851	2.444
0.25	6.443	3.806	2.637
0.27	6.653	3.795	2.857

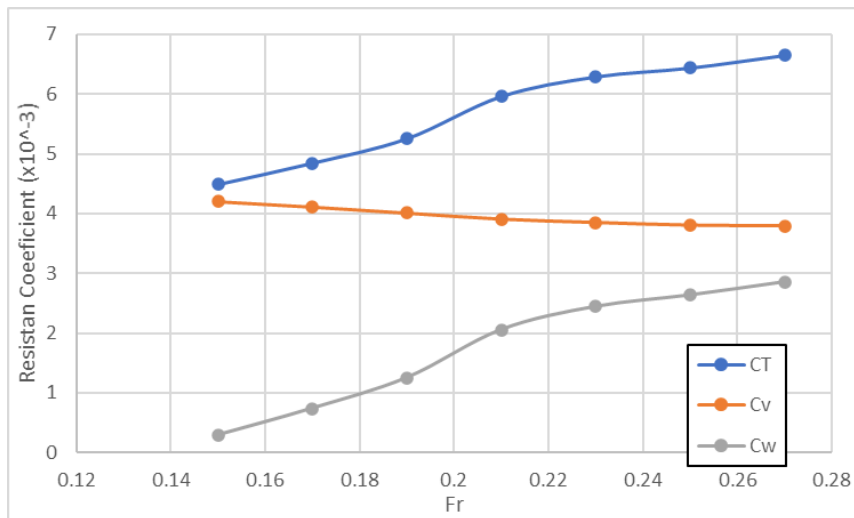
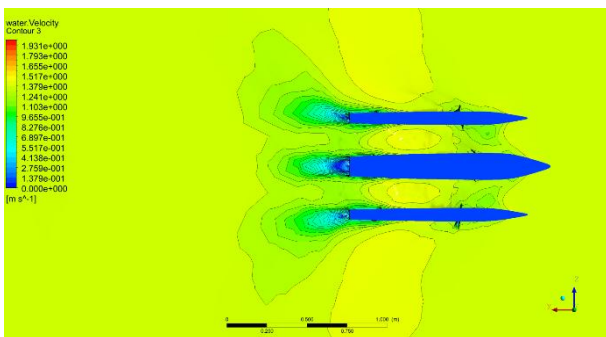
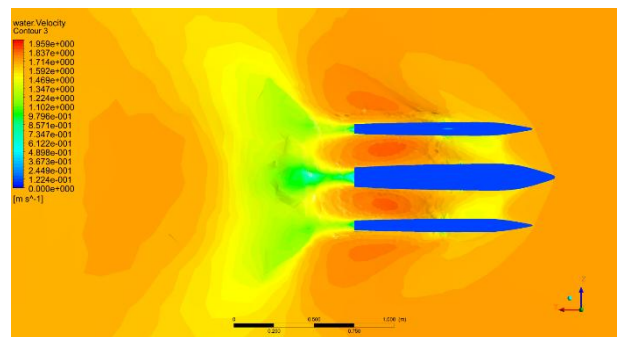


**FIGURE 5: Resistance Coefficient Trimaran Vessel**



(a)



(b)

**FIGURE 6: Trimaran Vessel, (a) Fr=0.21, (b) Fr=0.27**

The Engine Effective Power (EHP) calculation also shows the same trend, namely, trimaran vessels require the least power among other comparison vessels. This is shown in Figure 7. Where, the Trimaran ship at a speed of 12 knots requires a power of 608.08 kW, while the catamaran requires 629.16 kW power and the monohull ship requires 665.43 kW power. This shows the trimaran ship has the advantage of using less engine power. The shape of the flat hull or thin ship hull ( $L/B \gg$ ), the contribution of the resistance is greater than the wave resistance to the total resistance. Viscous resistance (which is dominated by friction resistance) increases with increasing hull length, Tuck and Lazauskas (1996). With the increase in the length or area of the wet area, the surface friction force will also increase. As for the wave resistance, in general, it becomes smaller as the length of the hull increases (for a fixed displacement).

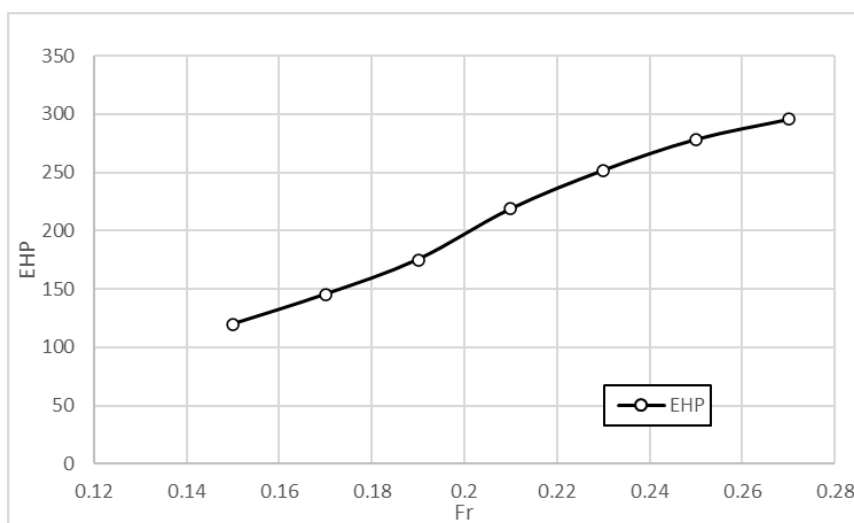


**FIGURE 7: Effective Horsepower**

### 3.2 Comfort and Safety

Ship comfort is indicated by the MSI measurement indication (Motion Sickness Index) which is determined by the remote location on the deck. Meanwhile, for the wave data and wave direction that has been calculated above.

In heading seas, MSI occurs in 10% of decks after 2 hours, on vehicle decks and decks. Where at that time the amount of encounter frequency was 1.666 Hz, and the vertical acceleration value was 0.503 m/s<sup>2</sup> on the crew deck. When the ship follows the waves, the ship is very stable, and it is predicted that no crew will experience seasickness. In the condition of the ship against the waves from the direction of 45 degrees, at the three measurement locations 10% of the crew will experience seasickness after 8 hours of voyage. And the highest cases are encountered frequencies of 0.508 Hz and vertical accelerations of 0.750 m/s<sup>2</sup>.

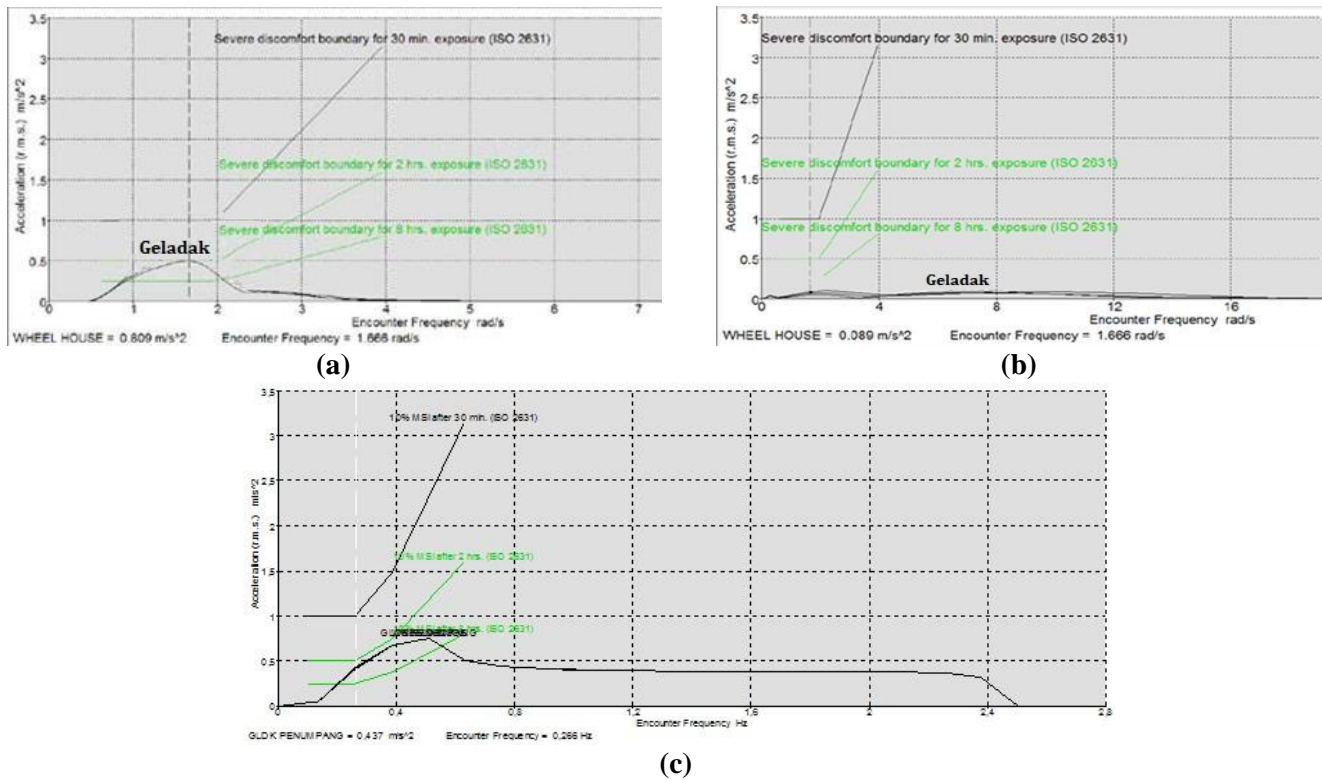


**FIGURE 8: MSI ships Trimaran S/L = 0.2, (a) Heading Seas (180°), (b) Following Seas (0°), (c) Quartering Seas (45°)**

According to the book Ship Stability for Mates and Masters, the period of shaking can be calculated by the formula:

$$T = \frac{2\pi CB}{\sqrt{gGM}} \tag{1}$$

Where :

T = Period

$$\begin{aligned} C &= 0.373+0.023(B/D)-0.043(LPP/100) \\ &= 0.373+0.023(10.4/2.85)-0.043(46/100) \\ &=0.437 \end{aligned}$$

B = Breadh

GM = Metacenter Point

The formula for moment of ship:

$$\begin{aligned} \text{Ship Momment} &= \text{Displacement} \times \text{GM} \\ &= 10.5 \text{ s} \end{aligned} \tag{2}$$

The shaking period for trimaran ships according to the International Maritime Organization (IMO) regulation is around 10 - 14.5 seconds, and the Trimaran IKan Ship has a shaking period of about 10.5 seconds so it still meets the IMO requirements.

#### IV. CONCLUSION

From the simulation results of the calculation of the Trimaran ship, several results can be concluded as follows.

1. Hull interference occurs as a visible change in speed between the flow velocity between the trimaran hull and those outside the hull.
2. The Trimaran ship has the highest vertical acceleration response when the ship is moving against the direction of the waves (heading seas), where at a ship speed of 15 knots, a wave height of 2.5 meters and an average wave period of 7.2 seconds causing vertical acceleration of  $0.806 \text{ m/s}^2$  respectively and  $0.503 \text{ m/s}^2$  on deck.
3. Shaking period of a trimaran is an average of 10.5 seconds, but on a trimaran that meets the IMO standard and is declared not good.

#### ACKNOWLEDGEMENTS

The author would like to thank Pattimura University for funding this research.

#### REFERENCES

- [1] Anderson, J.D., Jnr, 1995, Computational Fluid Dynamics, The basics with applications, McGraw-Hill International Editions.
- [2] ANSY CFX Manual VII, ANSYS 2015.
- [3] Baba, E.1996 A new component of viscous resistance of ships, Journal of the Society of Naval Architects of Japan, 125,23-34.
- [4] Bhattacharyya, Rameswar (1978). Dynamics of Marine Vehicles. John Wiley and Sons. USA.
- [5] Couser, P R, Molland, A F, Armstrong N and Utama, I K A P (1997), "Calm Water Powering Predictions for High Speed Catamarans", *Procs. Of International Conference on Fast Sea Transportation, FAST 1997, Sydney, 21-23 July*.
- [6] Couser, P R, Wellicome, J.F., Molland, A F. (1998), "An Improve Method for the Theoretical Prediction of the Wave Resistance of Transom-Stern Hulls Using A Slender Body Approach", *International Shipbuilding Progress, Vol. 45, No. 444*.
- [7] Hughes, G (1954), "Friction and Form Resistance in Turbulent Flow and a Proposed Formulation for Use in Model and Ship Correlation", *Trans INA, Vol. 96*.
- [8] Insel, M dan Molland, A F (1992), "An Investigation into the Resistance Components of High Speed Displacement Catamarans", *Trans RINA Vol. 134*.
- [9] ITTC (2002), *Recommended Procedures and Guidelines, Testing and Extrapolation Methods in Resistance Towing Tank Tests*, ITTC 7,5-02-02-02.
- [10] Kurultay, A.A.: 2003. Sensitivity analysis of the seakeeping behavior of trimaran ships. MScThesis, Naval Postgraduate School, Monterey, California (USA) (2003).
- [11] Luhulima R. B, Sutiyo, Utama I K A P . 2017. An Investigation Into The Correlation Between Resistance and Seakeeping Characteristics of Trimaran at Various Configuration and with Particular Case in Connection with Energy Efficiency. International Symposium on Marine Engineering (ISME) October 15-19, 2017, Tokyo, Japan
- [12] Menter, F.R. (1993), "Zonal Two Equation  $k-\omega$  Turbulence Models for Flows", *AIAA Paper 93-2906*.
- [13] Miyazawa, M. (1979), "A Study on the Flow Around a Catamaran", *Journal of Society of NavalArchitects of Japan*, No. 145, pp. 49 - 56.
- [14] Molland, A.F., Utama, I K A P., and Buckland, D. (2000), "Power Estimation for High Speed Displacement Catamarans", *The second Regional Conference on Marine Technology for*
- [15] Turner, H. dan Taplin, A. (1968), The Resistance of Large Powered Catamaran, Trans. SNAME, Vol. 76.
- [16] Utama, I K A P (1999), Investigation of the Viscous Resistance Components of Catamaran Forms, Ph.D Thesis, Department of Ship Science, University of Southampton, UK.
- [17] Utama, I K A P, Murdijanto dan Hairul (2008), An Investigation into the Resistance Characteristics of Staggered and Un-staggered Catamaran, RIVET, Kuala Lumpur – Malaysia, 15-17 Juli 2008
- [18] Zouridakis, F. (2005), A Preliminary Design Tools for Resistance and Powering Prediction of Catamaran Vessels, Master of Science Thesis in Ocean Systems Management, Dept. of Ocean Engineering, Massachusetts Institute of Technology.

# Effect of Citric Acid on Thickeners Used in Products for People Suffering Oropharyngeal Dysphagia

Josep García Raurich<sup>1</sup>, Anna Mas Herrador<sup>2</sup>, Queralt Pérez Ruiz<sup>3</sup>

Centre de Recerca en Seguretat i Control Alimentari (CRESCA), Universitat Politècnica de Catalunya, Spain

**Abstract**—Dysphagia is a digestive disorder recognized by the World Health Organization (WHO) in the International Classification of Diseases (ICD) characterized by the difficulty in forming or moving the bolus from the mouth to the oesophagus that can cause the passage of food into the respiratory tract. Foods for people with dysphagia are prepared with products that modify viscosity to make them safer when ingested. The aim of this work is to establish the interaction between citric acid, widely used by the food industry, with different thickeners, both first and second range, in order to check whether they fulfil the functions for which they have been designed. The time stability and viscosity as a function of the hydration time of six thickeners and their behavior in the temperature range between 25 and 50 °C were determined. Thickener concentrations up to a maximum of 6% were used in combination with 3 acid concentrations (0.5, 1 and 2%). In distilled water, the sedimentation of first range thickeners and the gelification of second range thickeners were checked, as well as the change from non-Newtonian to Newtonian behaviour after the hydrolysis process in both types of thickeners. In the presence of citric acid, the behaviour of both types of thickeners was analogous. Second range thickeners have been found to be much safer than first range thickeners in modifying the viscosity of liquids for people with dysphagia due to the fact that they do not sediment. .

**Keywords**—citric acid, dysphagia, gum, starch, thickener, viscosity.

## I. INTRODUCTION

Pulmonary aspiration is the passage of material generated in the stomach, esophagus, mouth or nose from the pharynx to the trachea and lungs. When this passage of material is related to the difficulty in moving food from the mouth to the stomach, it is known as dysphagia [1].

Dietary modifications should be individualized according to the type of dysfunction and the chewing and swallowing capacity of each patient. Thus, different consistency degrees have been standardized so that the patient can have the optimal diet and eat correctly ensuring that nutritional and water requirements are achieved. Consequently, the diet may vary from liquid to solid, through different degrees of consistency [2].

Although patients are sometimes unaware of the disorder, oropharyngeal dysphagia is a very common clinical condition, affecting more than 30% of stroke patients, 60-80% of patients with neurodegenerative diseases, 10-30% of adults over 65 years of age and more than 51% of elderly institutionalized patients [3].

Fluids are usually thickened to slow down their transit speed, to avoid aspiration of material into the respiratory tract and to improve transit into the oesophagus. However, names, level number of modification and characteristics vary within and between countries. In fact, over the past 30 years, as knowledge of dysphagia has grown, more technical definitions have emerged that delineate the difference between oesophageal and oropharyngeal dysphagia [4].

In October 2012, at the meeting of the European Swallowing Disorder Society in Barcelona, an initiative was developed that aims to achieve an international standardised terminology and definitions for textured modified foods and thickened liquids for individuals with dysphagia of all ages, in all care settings and all cultures. The result of this meeting was the formation of the International Dysphagia Diet Standardisation Initiative (IDDSI) [5].

In the experimental development of this publication, the classification of The National Dysphagia Diet (NDD) has been used, which is a way of objectifying the different degrees of consistency of diets through viscosity[6]. Thus, four categories of viscosity are distinguished:

- a) Thin viscosity, water and beverages in general (1-50 cP);
- b) Nectar viscosity, allows ingestion in the form of sips (51-350 cP)
- c) Honey viscosity, allows ingestion with a spoon, and does not maintain its original shape and consistency (351-1750 cP)
- d) Pudding viscosity, allows ingestion with a spoon, maintains its shape and consistency and cannot be drunk (>1751 cP).

In recent decades, there has been a rapid development of thickening agents used in the treatment of dysphagia. Initially, food-based thickeners such as potato starch, maize flour and rice cereal were used. Later, modified maize starch gained popularity, but more recently gums-based thickeners have become more popular due to their stability over time [7]. However, starch-based thickeners may not dissolve well in some liquids, may appear cloudy and may continue to thicken over time [8].

On the other hand, rubber-based thickeners appear to offer some advantages over starch-based products [9]. Unlike starch, gums (including xanthan gum) do not degrade with the amylase in the saliva, which allows the viscosity to remain stable. They are supposed to reach the desired viscosity quickly, which makes them very suitable for hot drinks, and have been shown to maintain stability in liquids over time [10].

Nowadays, a distinction is made between two types of thickeners, those containing starch and those not containing starch, although, in the first group, a distinction is usually made between those consisting only of starch and those that are mixtures of starch, and gums [11]. This type of thickener is called first-range and usually uses modified maize starch or a maltodextrin derived from maize.

Second-range thickeners are composed exclusively of gums and in some particular cases may contain a small amount of modified starch. They differ from the first range in that the amount of product to be used to obtain the desired viscosity is considerably lower.

The aim of this manuscript is to establish the influence of citric acid (E 330) on six commercial thickeners of plant origin. Based on previous experiences, it was determined at different concentration values: the temporal stability of the recently prepared samples; the Newtonian or non-Newtonian behaviour as a function of the rest time and its behaviour in the temperature range between 25 and 50°C [12, 13].

## II. METHODOLOGY

The behaviour of six thickeners was determined, two of them first-range: Densiter® y Resource®; and four second-range: ViscoInstant®, Fresubin®, Clinutren® and Gelcarin®. The behaviour of these thickeners was studied in a neutral medium with distilled water and in an acid medium with citric acid. Citric acid (supplied by PANREAC with a degree of purity for analysis) was used for this purpose.

Samples were prepared at different concentrations of each thickening product in order to obtain samples of the four degrees of consistency accepted in the oropharyngeal dysphagia field (thin liquid, nectar, honey and pudding). At the same time, the concentration of citric acid was also modified for each concentration of thickening product. The acid concentrations studied were 0.5, 1 and 2%. The samples used had a volume of 650 mL and were prepared in triplicate expressing the concentration of thickener in % by weight. TABLE 1 shows the composition of each thickener used in this work.

**TABLE 1**  
**THICKENERS COMPOSITION**

Product	Type	Origin	Composition
Densiter®	First range thickener	Plant	Corn starch
Resource®		Plant	Modified corn starch
Viscoinstant®	Second range thickener	Plant	Maltodextrin, xanthan gum and guar gum.
Clinutren®		Plant	Maltodextrin, xanthan gum, potassium chloride and may contain traces of milk
Gelcarin®		Plant	Carrageenan, potassium citrate and sucrose
Fresubin®		Plant	Modified tapioca starch, xanthan gum, maltodextrina, modified cellulose and natural aroma.

In the first-range thickener the formation of lumps was observed. Lumps are an added problem in the preparation of food for patients with dysphagia as they can cause problems in swallowing. To avoid as much as possible the formation of lumps, once the solvent (distilled water or citric acid solutions) was prepared, a constant agitation was maintained at 1000rpm while slowly pouring the thickener to be studied at room temperature.

The main objective of this project was to determine the viscosity at different temperatures of freshly prepared samples and after a 5-hour rest period. The temperature range was between 25 and 50°C and the different experimental series differed by 5°C.

Viscosities matching a thin viscosity, below 30 cP, were determined using a pre-calibrated Cannon Fenske 520 Viscometer, while for the remaining viscosity determinations a pre-calibrated Brookfield RTV31196 Rotational Viscometer was used. In



the case of the Cannon Fenske viscometer, it was imposed as a restrictive criterion that the difference between two consecutive measurements of the same sample should not exceed one second. Otherwise, the measurement was repeated. When operating the Brookfield RTV 31196 viscometer, the criterion imposed was to accept a maximum dispersion value of 3% between two consecutive measurements [14]. The temperature of the samples was regulated with the aid of a Lauda E100 thermal bath. Once the measurements had been made on the freshly prepared samples, they were kept in refrigeration at 4°C and the tests were repeated after 5 hours. The various samples were prepared by weighing the corresponding solute with a Scaltec SBC 33 analytical balance. A JW-3510 pH meter previously calibrated at the beginning of each session was used for the determination of pH. Three readings were taken once the sample was stabilized and the average value of the three readings was taken into account. Fig. 1 shows the block diagram followed during this process.

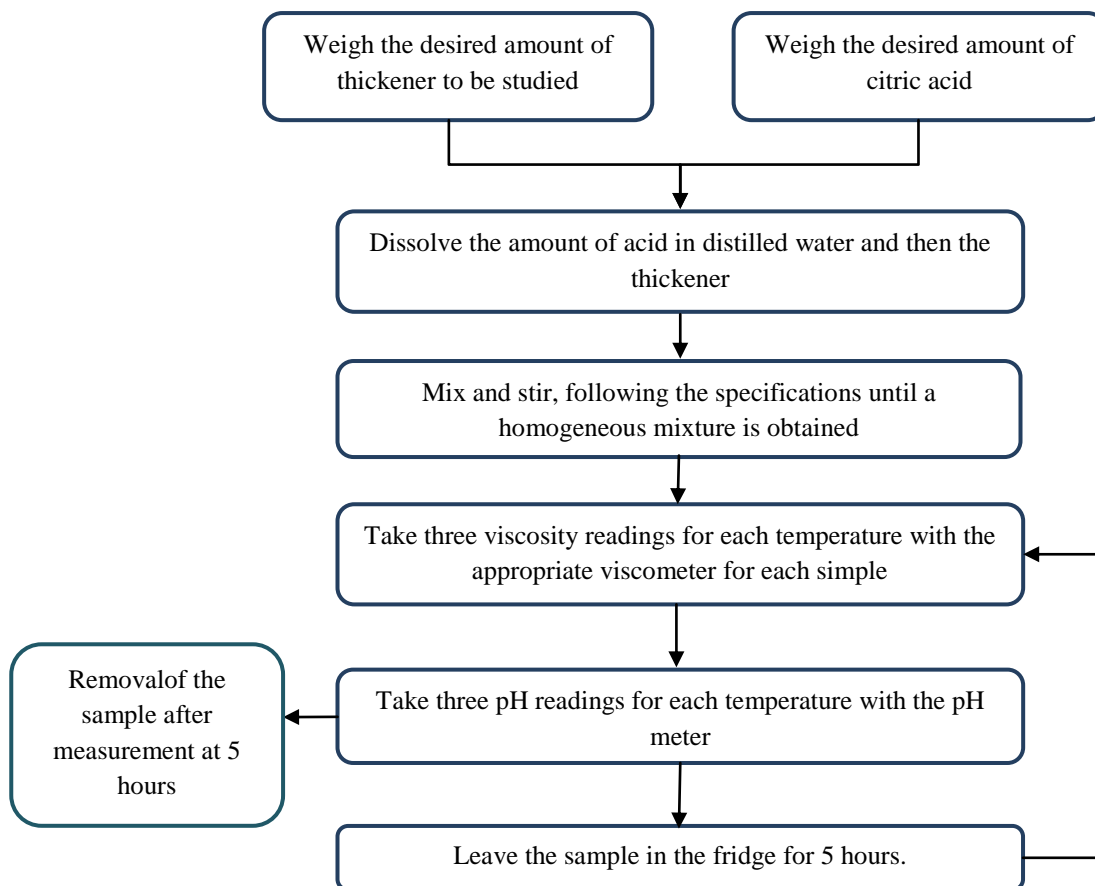


**FIGURE 1: Sample preparation process**

### III. RESULTS

#### 3.1 Temporal stability of the samples

The viscosity of the different thickeners was determined after the corresponding sample was homogenised. This homogenisation was necessary because a sedimentation process was observed in the samples of the two first-range thickeners, Densiter® and Resource®. This sedimentation was not observed in the samples of the second range thickeners, which remained stable indefinitely, forming gels.

Confirmation that this behaviour was due to the presence of starch was made through the Lugol test (iodine solution). For this purpose, samples were prepared at 1% of each thickener and the experiment was carried out at two temperatures, 25 and 90°C.

As can be seen in Fig. 2, a positive result was obtained for the presence of starch in the first range thickeners. The result was in line with the composition of Densiter® (native starch) and Resource® (modified starch). The same intense colouring was obtained in the Clinutren® second range thickener, despite the fact that the technical data sheet for this thickener does not indicate the presence of starch (this unexpected behaviour was interpreted as an interference of the type of maltodextrin used).

The Viscoinstant® and Fresubin® thickeners showed a slight colouration indicating signs of starch. The technical data sheet for Fresubin® thickener does indicate the presence of starch, whereas for Viscoinstant® thickener there is no reference to the incorporation of this carbohydrate. Gelcarin® thickener showed a yellowish colouring in Lugol's test which does not indicate the presence of starch as indicated in its technical data sheet.

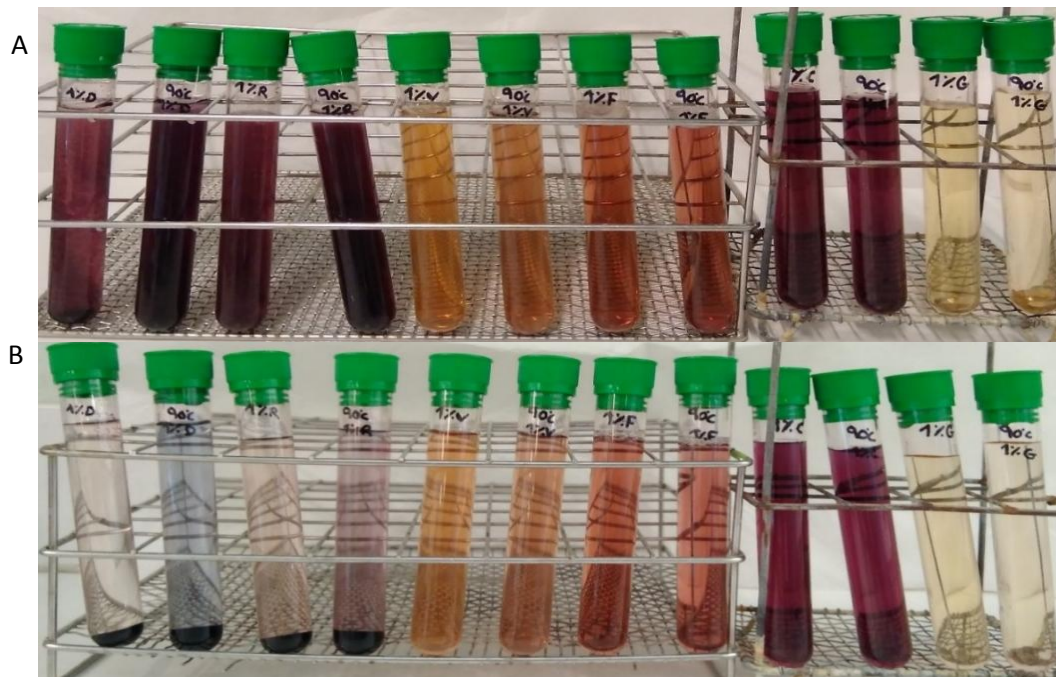


**FIGURE 2: Lugol test with a concentration of 1% of all thickeners at 25°C and 90°C:a) Just performed b) Left to stand.**

Only the samples of Densiter® and Resource® thickeners precipitated at both 25 and 90°C, while the rest of the Viscoinstant®, Fresubin®, Clinutren® and Gelcarin® thickeners did not. Consequently, it can be concluded that they only sediment the first-range thickeners when left to stand, as a result of the high percentage of starch present in their composition.

### 3.2 Degrees of consistency

The results obtained experimentally were structured according to the different degrees of consistency accepted by the (NDD) [6]. TABLE 2 shows the results obtained for each thickener.

**TABLE 2  
CONSISTENCY AS A FUNCTION OF CONCENTRATION.**

	Type of Thickener	Thin Liquid 1-50 CP	Nectar 51-350 CP	Honey 351-1750 CP	Pudding>1751 CP
<b>Densiter®</b>	1st gamma	≤ 3%	4%	5%	≥ 6%
<b>Resource®</b>	1st gamma	≤ 3%	4%	5%	≥ 6%
<b>Fresubin®</b>	2nd gamma	< 0,3%	[0,3%-1%]	[2% - 3%]	≥ 3%
<b>Viscoinstant®</b>	2nd gamma	≤ 0,3%	0,5%	[1% - 2%]	≥ 3%
<b>Clinutren®</b>	2nd gamma	≤ 0,3%	[0,5%-1%]	[2% - 4%])	≥ 4%
<b>Gelcarin® (*)</b>	2nd gamma	---	---	---	---

*(\*) Compound containing carrageenan. In the samples just prepared, the degree of consistency was always a thin. After being left to stand, it was systematically changed to honey or pudding consistency.*

As expected, as the concentration of thickener increased, the degree of consistency (viscosity) increased. However, first and second range thickeners behaved significantly differently: second range thickeners needed less thickener to reach the same degree of consistency. In fact, for the thin liquid and nectar consistency, 10 times more of a first-range thickener was needed

than a second-range thickener; for the honey consistency, 2.5 times more was needed and for the pudding consistency, twice as much as a second-range thickener was needed.

### 3.2.1 Thin liquid

A thin liquid consistency of up to 3% by weight was achieved with the first-range thickeners Densiter® and Resource®. In contrast, with the second-range thickeners Viscoinstant®, Clinutren® or Gelcarin®, this consistency was achieved only with a percentage of less than 0.3%. All thickeners prepared with distilled water in the thin liquid consistency showed a Newtonian behaviour, i.e. as the temperature increased the experimental value of the viscosity decreased.

When the thickeners were left to stand for 5 hours, the samples with the first-range thickeners showed higher viscosity values than the freshly prepared samples. This is the opposite of the second range thickeners which, when left to stand for 5 hours, presented lower absolute values of viscosity, with the exception of the Gelcarin® thickener whose composition is based on carrageenan and not on xanthan gum. In all cases, the viscosity values decreased with temperature, after the resting period. Fig. 3 shows the behaviour of a first-range thickener, Densiter®, and a second-range thickener, Viscoinstant®.

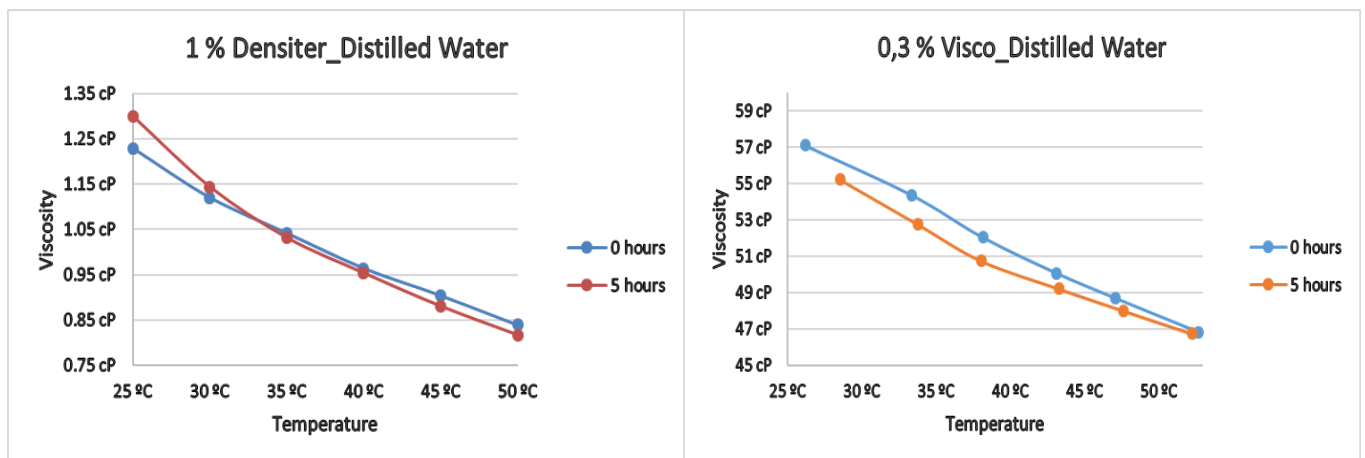


**FIGURE 3: Newtonian viscosity behaviour in the same samples without and with a rest period, Densiter®: first-range thickener; ViscoInstant®: second-range thickener.**

### 3.2.2 Nectar consistency

Samples of nectar consistency with first-range thickeners showed a non-Newtonian behaviour at 0 hours and a Newtonian behaviour in the same samples left at rest for 5 hours (Fig. 4). In contrast, all the samples with second-range thickeners showed a Newtonian behaviour independently of the rest time.

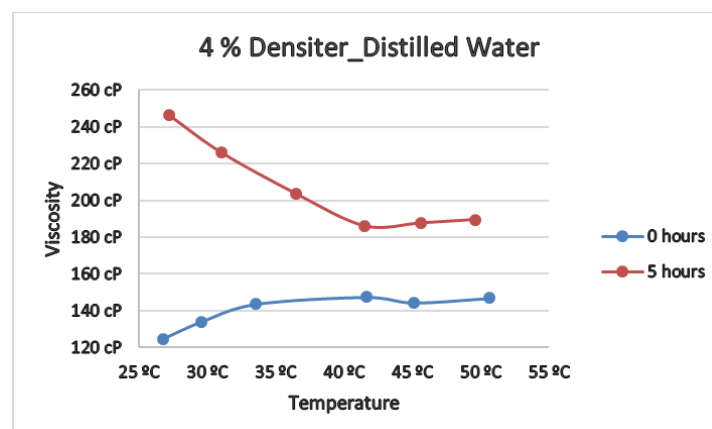


**FIGURE 4: Evolution from non-Newtonian behaviour, without a rest period, to Newtonian, with a rest period, from Densiter® first-range thickener at a concentration of 4%.**

### 3.2.3 Honey consistency

The samples just prepared with first-range thickeners showed a non-Newtonian behaviour and these same samples, left to stand for 5 hours, showed a Newtonian behaviour. Fig. 5 shows the behaviour of Densiter® at 5%.

In relation to the behaviour of the second-range thickeners, each thickener presented a different singularity. Thus, Viscoinstant® showed a non-Newtonian behaviour in the newly prepared samples. However, after 5 hours of rest, it showed a Newtonian behaviour up to a temperature of 40°C. However, at higher temperatures its behaviour was no longer Newtonian.

Regarding Clinutren®, the recently prepared samples showed a non-Newtonian behaviour up to a temperature of 45°C and up to 40°C the samples left to stand for 5 hours. The Gelcarin® thickener showed a particular behaviour in comparison with the other thickeners: in the samples just prepared it always presented low viscosities that corresponded to the consistency of a thin liquid. On the other hand, when it was left to stand at low temperatures, its viscosity increased drastically to a honey consistency with a concentration of 0.75% by weight. When the sample was subjected to increases in temperature, its viscosity decreased again to a fine liquid consistency (see Fig. 5).

Finally, Fresubin® behaved more clearly than Clinutren®, showing a non-Newtonian behaviour up to 35°C in freshly prepared samples and up to 40°C in samples left to stand for 5 hours.

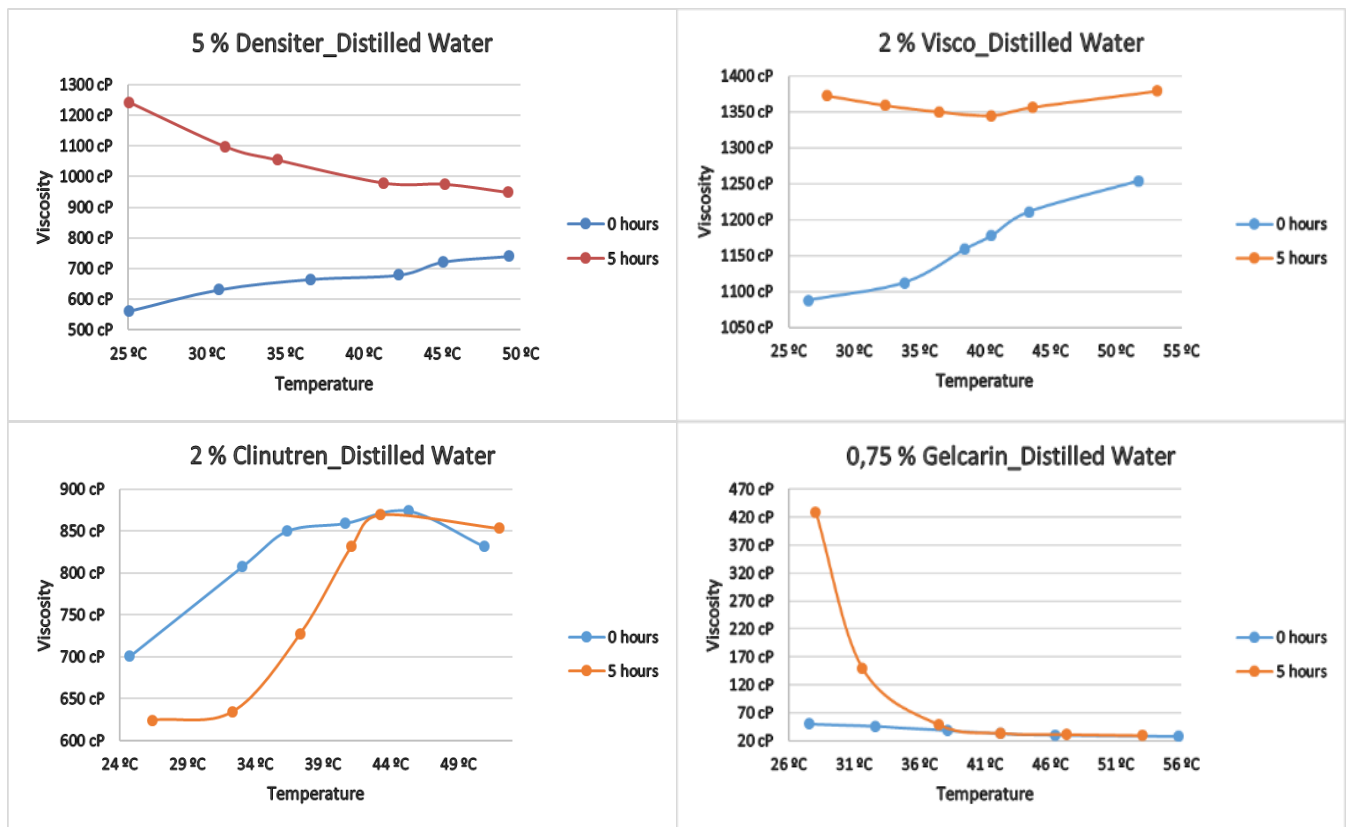


**FIGURE 5: Evolution of viscosity behaviour of Densiter®, Viscoinstant®, Clinutren® and Gelcarin® thickeners in the degree of honey consistency without and with a rest period.**

### 3.2.4 Pudding consistency

All the samples prepared with pudding consistency showed a non-Newtonian behaviour, i.e. the viscosity increased with increasing temperature, with the exception of the sample with Gelcarin®. This thickener, with a concentration of 1%, increased its viscosity, from a thin liquid to a pudding consistency, after the resting period. Its behaviour was practically identical to that observed with a concentration of 0.75% and a honey consistency (Fig. 5).

The samples left to stand for 5 hours of the first range thickeners, Densiter® and Resource®, showed Newtonian behaviour, unlike the second range thickeners Viscoinstant®, Clinutren® and Fresubin® which showed non-Newtonian behaviour.

### 3.3 Interaction of citric acid

Citric acid modified the behaviour of thickeners. The degree of interaction was different in the first-range thickeners from the second-range ones.

### 3.3.1 Thin liquid

Freshly prepared samples with a thin liquid consistency changed their behaviour due to the introduction of citric acid. First-range thickeners increased the absolute viscosity values, in contrast to second-range thickeners, which decreased these values.

All the samples with the consistency of a thin liquid, when they were left to stand, showed a Newtonian behaviour regardless of the thickener considered. However, the first range thickeners in the presence of acid increased the absolute values of viscosity, while the second range thickeners decreased the absolute values of viscosity. Fig. 6 shows the evolution over time of a first range thickener, Densiter®, and a second range thickener, Viscoinstant®.

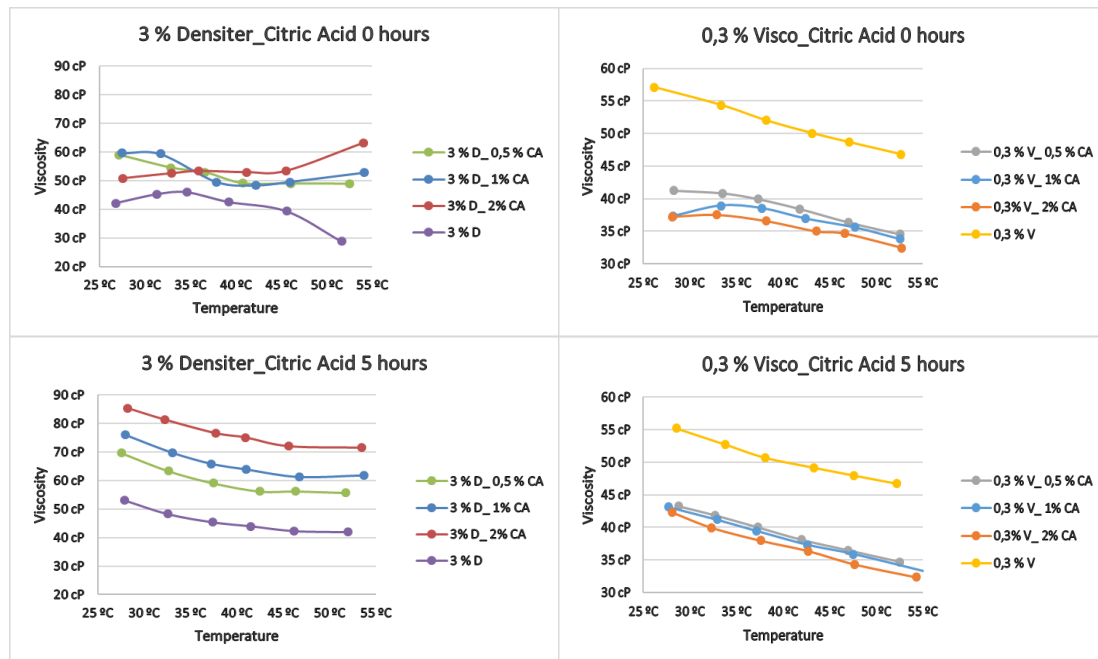


**FIGURE 6: Viscosity evolution as a function of temperature and time in samples under the influence of citric acid.**

### 3.3.2 Nectar consistency

The behaviour of the samples just prepared with both types of thickeners in the presence of acid was modified with respect to the samples prepared with distilled water, analogous to the case of the consistency of thin liquid: increase in the absolute values of viscosity in the samples with first-range thickeners and decrease in the second-range.

When the samples were left to stand for 5 hours, all the experimental data series showed a Newtonian behaviour and it was confirmed that the presence of acid in the samples prepared with first range thickeners increased the absolute values of viscosity while in the samples of second range thickeners the viscosity decreased.

### 3.3.3 Honey consistency

The samples with honey consistency just prepared with Densiter® and Resource® first-range thickeners in the presence of citric acid showed a non-Newtonian behaviour. On the other hand, the samples prepared with the second-range thickeners Viscoinstant® and Clinutren® showed a Newtonian behaviour, whereas the samples prepared with Gelcarin® and Fresubin® showed a unique behaviour, the last one due to its carrageenan-based composition (Fig. 7).

After the 5-hour rest period, Newtonian behaviour was observed in all cases. Furthermore, with the exception of Gelcarin®, the increase in the absolute values of viscosity was confirmed, which determined a change in the behaviour of the thickeners of the second range with respect to that observed in the degrees of thin liquid and nectar consistency.

### 3.3.4 Pudding consistency

The pudding consistency samples just prepared with first-range thickeners in the presence of citric acid showed a non-Newtonian behaviour. When acid was introduced in the samples just prepared with second-range thickeners, they showed a



Newtonian behaviour, as it had been observed in the honey consistency. Again, with the exception of Gelcarin®, the presence of acid increased the absolute values of viscosity in all cases.

Once the 5 hour rest period was over, a Newtonian behaviour was observed in all cases, confirming the increase in the absolute values of viscosity with acid, with the exception of the samples prepared with the Gelcarin® thickener. It was confirmed that, when the samples were left to rest, they increased their tendency towards a Newtonian behaviour.

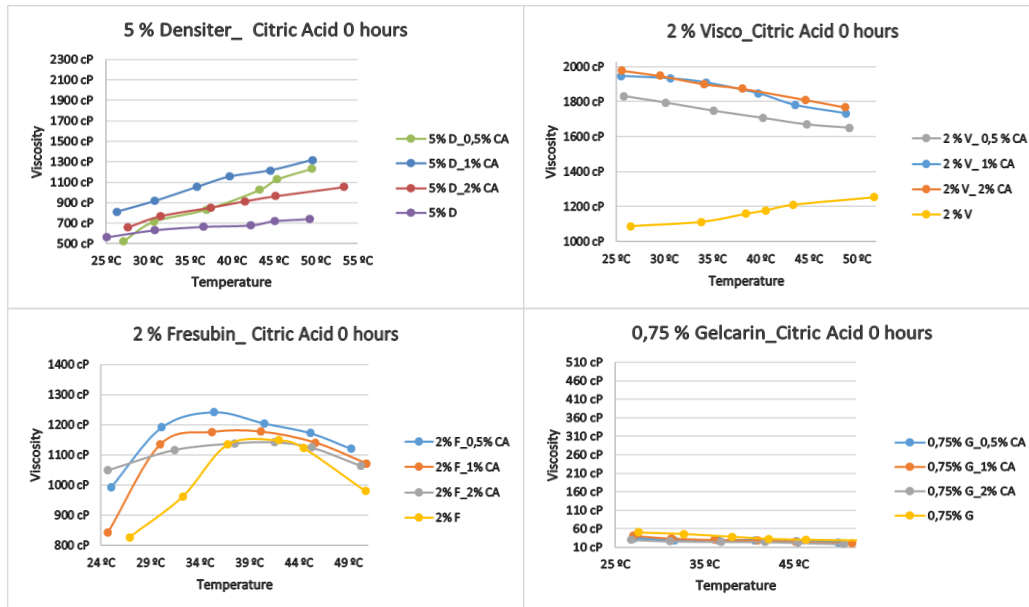


**FIGURE 7: Influence of citric acid on samples just prepared with honey consistency.**

### 3.4 pH behaviour study

The possible correlation of pH with viscosity values at different temperatures was studied in order to establish an effect of the acidic environment on the hydration process of thickeners.

Fig. 8 shows that the pH has no direct relation with the variation of the viscosity values. The behaviour of Gelcarin® is shown, the only thickener that presented pH values in the alkaline zone when it was dissolved with distilled water and the behaviour of Fresubin® in the honey consistency. No significant variations of pH are observed compared to the resting time of the samples. This behaviour was observed in all the samples, independently of the thickener used.

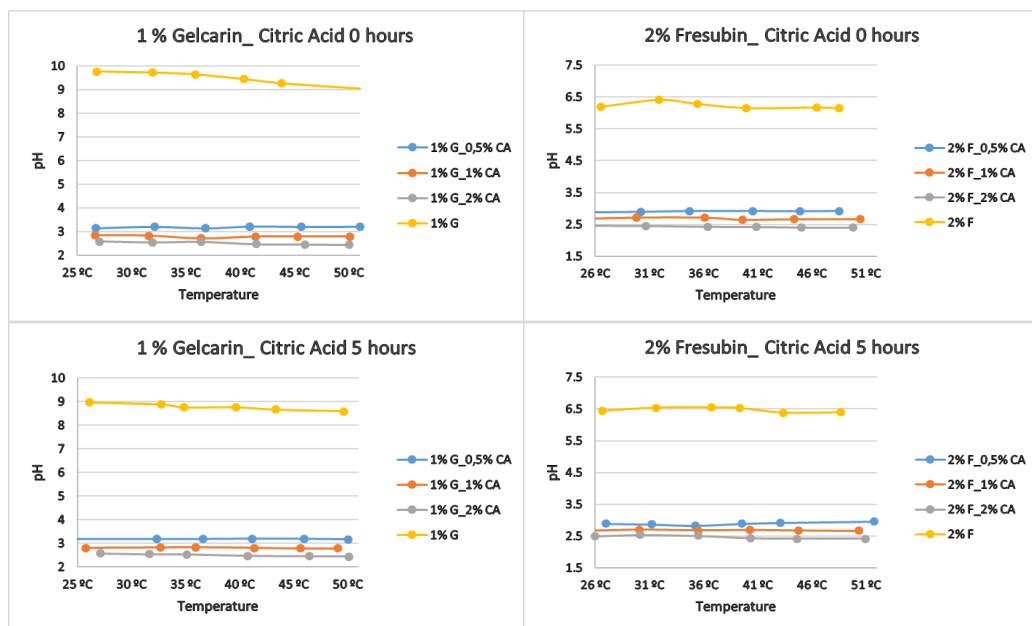


**FIGURE 8: pH values in just prepared samples and left to stand for 5 hours of Gelcarin® and Fresubin®.**

#### IV. DISCUSSION

Substances with the ability to form a gel have been used in the production of processed foods for a long time [15], examples being starch of plant origin and gelatine of animal origin. Chemically complex substances are also used, obtained either from plants or from micro-organisms that are indigestible by the human organism [16,17]. Thus, for example, the unique biophysical properties of alginate, carrageenan and agar are very valuable in the development of functional food products. As food ingredients, the thickening, gelling and emulsifying properties are particularly useful in the application of seaweed hydrocolloids in foodstuffs [18]. In general, stabilisers have functional properties that are closely related to their capacity to retain and conserve large quantities of water, which influences the modification of the rheological characteristics of the mixtures [19,20].

The use of thickeners and reduction of intake volumes in patients with dysphagia is a common practice, and an improvement is observed when changing from a fluid consistency (water) to a thicker one (nectar, honey, pudding) [21]. For the functional properties of thickeners to be observed they must be hydrated in water. For effective hydration, it is first necessary to ensure that all the individual particles that make up the dry powder are quickly separated from each other when the water phase is added. Many thickener solutions are pseudoplastic and each has its own characteristics [22,23].

Commercial thickeners used in the treatment of dysphagia present different properties when dispersed in different liquids such as water, coffee, milk or juice [24, 25], influencing sensory perception [26-29].

Although thickeners based mainly on granulated maize starch are widely used in the care of patients with swallowing difficulties, it has been shown that thickened fluids show behaviour that varies over time and are not Newtonian since starch-based thickeners cause a liquid to thicken as the starch molecules swell (hydrate). In contrast, gum-based thickeners cause tangled webs in which water molecules are enclosed [30,31].

In view of the results obtained in this study, it is not recommended to use top-of-the-range thickeners for the treatment of dysphagia due to their sedimentation. This sedimentation took place even in samples treated at 90°C and was attributed to starch. On the contrary, the second range thickeners gelled resulting in stable gels, results in line with the literature consulted. Other limitations of first-range thickeners were: the formation of lumps and the need for a greater quantity of product to reach the same degree of consistency as second-range thickeners.

Each thickener behaved differently depending on its composition. Moreover, the second range thickeners also showed differences in their behaviour. For instance, Gelcarin® thickener went from a thin liquid consistency to pudding thick and vice versa very quickly depending on the temperature, after a period of rest. This unique behavior is due to the fact that it contains carrageenan – E 407- as the main component. This behaviour is not recommended for patients with dysphagia and is analogous to that described for gelatine [12]. On the other hand, Fresubin® thickener produced foam, behaviour that was associated with the presence of modified cellulose, while Viscoinstant® and Clinutren® thickeners showed similar behaviour due to a very similar composition.

In the presence of citric acid, the absolute values of the viscosities of all thickeners were affected. Unlike the pH values which, for practical purposes, remained constant at variations in temperature and time even in the case of Gelcarin® whose initial pH is in the alkaline zone (the addition of the acid caused a neutralisation of this thickener). That is to say, it was observed that the viscosities of the various thickeners used were not affected by the pH, coinciding with that observed in [32].

In relation to the degree of consistency, the various thickeners showed Newtonian behaviour in samples of thin liquid, i.e. the experimental value of the viscosity decreased as the temperature increased. This behaviour was observed both in the just prepared samples and after a 5-hour rest period.

In the second range thickeners a Newtonian behaviour was also observed in the samples with nectar consistency in all cases. On the other hand, in the samples just prepared with a first range thickener and nectar consistency, a non-Newtonian behaviour was observed, i.e. as the temperature increased, the experimental value of viscosity increased.

For the degree of honey consistency each thickener followed a singular behaviour trend and for the degree of pudding consistency the second range thickeners followed a non-Newtonian behaviour when prepared with distilled water. In all cases, the absolute values of viscosity were higher in the presence of citric acid.



The change in behaviour in the samples just prepared in relation to the samples left at rest was interpreted as proof of the completion of the hydration process of the different thickeners. This hydration was found to be reached after 5 hours in all the cases considered in this study.

The results obtained show that the viscosity of water with commercial thickeners is affected to varying degrees depending on whether they are first or second range. Likewise, the addition of acids, salts or sugars causes a change in their behaviour which can affect the swallowing capacity of the resulting mixtures [33-35].

## V. CONCLUSIONS

There is a direct correlation between the concentration of thickener and the degree of consistency. This fact indicates that rigorous monitoring of the relevant indications is required when preparing a standard sample since, if no rigorous action is taken, there is a risk of aspiration into the lung.

First range thickeners sediment when left to rest as a result of the high percentage of starch present in their composition. As the temperature increases, the starch swells and thickens, while the hydrocolloids containing gums in their composition (especially xanthan) remain stable.

So called second-range thickeners, which are made exclusively of gums and in some particular cases may contain a small amount of modified starch, allow a significantly lower amount of product to be used to obtain the desired viscosity, especially in the nectar and honey consistency grades, so that the visual appearance and taste of the thickened liquid is modified to a lesser extent.

It is proposed to extend the study of the interaction of thickeners with other food substances in order to achieve their purpose.

## REFERENCES

- [1] Zargaraan A, Rastmanes R, Fadavi G, Zayeri F, Mohammadifar M. Rheological aspects of dysphagia-oriented food products: A mini review, *Food Sci. Hum. Wellness*. 2013;2(3-4):173-178. <http://dx.doi.org/10.1016/j.fshw.2013.11.002>.
- [2] [Cichero J, Lam P. Thickened Liquids for Children and Adults with Oropharyngeal Dysphagia : the Complexity of Rheological Considerations. *J. Gastroenterol. Hepatol. Res.*2014;3(5):1073–1079. doi:10.6051/j.issn.2224-3992.2014.03.408-13.
- [3] Ortega O, Martín A, Clavé P. Diagnosis and Management of Oropharyngeal Dysphagia Among Older Persons, State of the Art. *J. Am. Med. Dir. Assoc.* 2017;18(7):576–582. <http://dx.doi.org/10.1016/j.jamda.2017.02.015>.
- [4] [Cichero J. Thickening agents used for dysphagia management: effect on bioavailability of water, medication and feelings of satiety. *Nutr. J.* 2013;12(54):1–8. doi:10.1186/1475-2891-12-54.
- [5] Cichero J et al. The Need for International Terminology and Definitions for Texture-Modified Foods and Thickened Liquids Used in Dysphagia Management: Foundations of a Global Initiative. *Curr. Phys. Med. Rehabil. Reports*, 2013;1(4):280–291, DOI 10.1007/s40141-013-0024-z.
- [6] Dysphagia Diet Task Force. National Dysphagia Diet: Standardization for Optimal Care. Chicago, IL: American Dietetic Association; 2002.
- [7] Clavé P, De Kraa M, Arreola V, et al. The effect of bolus viscosity on swallowing function in neurogenic dysphagia. *Aliment Pharmacol Ther.* 2006; 24(9):1385-1394. DOI: 10.1111 / j.1365-2036.2006.03118.x.
- [8] Mertz Garcia J, Chambers E, Matta Z, Clark M. Viscosity measurements of nectar- and honey-thick liquids: Product, liquid, and time comparisons. *Dysphagia.* 2005; 20(4):325-335. DOI: 10.1007 / s00455-005-0034-9.
- [9] Vilardell N, Rofes L, Arreola V, Speyer R, Clavé P. A comparative study between modified starch and xanthan gum thickeners in post-stroke oropharyngeal dysphagia. *Dysphagia.* 2016;31:169–179. DOI: 10.1007 / s00455-015-9672-8.
- [10] Hanson B, O’Leary MT, Smith CH. The effect of saliva on the viscosity of thickened drinks. *Dysphagia.* 2011;27(1):10-19. DOI: 10.1007 / s00455-011-9330-8.
- [11] Irlés J, García-Luna P, El menú de textura modificada; valor nutricional, digestibilidad y aportación dentro del menú de hospitales y residencias de mayores. *Nutr Hosp.* 2014;29(4):873-879. DOI:10.3305/nh.2014.29.4.7285.
- [12] García M, García J, Raventós M, Alba M. Viscosidad en la dieta de pacientes diagnosticados de disfagia orofaríngea. *Acta Bioquím Clín Latinoam* 2016; 50 (1): 45-60.
- [13] García M, García J, Raventós M, Marceló S. Interacción de la glucosa con espesantes utilizados en el control de la disfagia orofaríngea *Acta Bioquím Clín Latinoam* 2017; 51 (4): 637-652.
- [14] ISO2555:1989. Plastics-Resins in the liquid state or as emulsions or dispersions. Determination of apparent viscosity by the Brookfield Test method.
- [15] Biliaderis C. The structure and interactions of starch with food constituents. *Canadian Journal of Physiology and Pharmacology.* 1991. 60: 60-78. DOI: 10.1139/y91-011.
- [16] Sahay D, Bhattacharva S. Hydrocolloids as thickening and gelling agents in food: a critical review. *J Food Sci Technol.* 2010; 47 (6): 587–597. DOI: 10.1007 / s13197-010-0162-6.
- [17] Martínez, O., Vicente, M. S., De Vega, M. C., & Salmerín, J. Sensory perception and flow properties of dysphagia thickening

- formulas with different composition. *Food Hydrocolloids*. 2019; 90:508–514. doi:10.1016/j.foodhyd.2018.12.045.
- [18] Qin Y. Seaweed Hydrocolloids as Thickening, Gelling, and Emulsifying Agents in Functional Food Products. *Bioactive Seaweeds for food applications*. 2018, 135-152 <https://doi.org/10.1016/B978-0-12-813312-5.00007-8>.
- [19] Park SH, Hong GP, Kim JY, Choi MJ, Min SG. The influence of Food Hydrocolloids on Changes in the Physical Properties of Ice cream. *Food Science Biotechnol* 2006 15 (5); 721-7.
- [20] Larsen, B.E, Bjørnstad, J, Pettersen, E.O. Rheological characterization of an injectable alginate gel system. *BMC Biotechnology*. 2015;15, 29–40. DOI 10.1186/s12896-015-0147-7.
- [21] Moret-Tatay, A, Rodríguez-García, J, Martí-Bonmatí, E, Hernando, I, & Hernández, M. J. Commercial thickeners used by patients with dysphagia: Rheological and structural behaviour in different food matrices. *Food Hydrocolloids*. 2015;51:318–326. doi:10.1016/j.foodhyd.2015.05.019.
- [22] O'Leary M, Hanson B, Smith C. Viscosity and non-Newtonian features of thickened fluids used for dysphagia therapy. *J Food Sci* 2010 1;75(6); 330-8. doi: 10.1111/j.1750-3841.2010.01673.x.
- [23] González-Bermúdez, C. A., Castro, A., Perez-Rea, D., Frontela-Saseta, C., Martínez-Graciá, C., Nilsson, L. Physicochemical properties of different thickeners used in infant foods and their relationship with mineral availability during in vitro digestion process. *Food Research International*. 2015;78:62–70. doi:10.1016/j.foodres.2015.11.006.
- [24] Sopade P, Liang S, Halley J, Cichero J, Ward L. Moisture absorption characteristics of food thickeners used for the management of swallowing dysfunctions. *European Food Research and Technology*. 2007. 224:555-560. <https://doi.org/10.1007/s00217-006-0325-x>
- [25] Hernández J, Correa M, Vial R, Forcano M, Gómez R, González P. How to prescribe for patients with dysphagia: a review for the adaptation of the pharmaceutical guide in a socio-sanitary hospital Farm Hosp. 2013. 37 (3):198-208. DOI: 10.7399/FH.2013.37.3.577.
- [26] Martínez, O., Vicente, M. S., De Vega, M. C., & Salmerín, J. Sensory perception and flow properties of dysphagia thickening formulas with different composition. *Food Hydrocolloids*. 2019; 90:508–514. doi:10.1016/j.foodhyd.2018.12.045
- [27] Ong, J. J.-X, Steele, C. M, Duizer, L. M. Sensory characteristics of liquids thickened with commercial thickeners to levels specified in the International Dysphagia Diet Standardization Initiative (IDDSI) framework. *Food Hydrocolloids*. 2018; 79: 208–217. doi:10.1016/j.foodhyd.2017.12.035.
- [28] Kim, Y., Kim, Y.-S., Yoo, S.-H., & Kim, K.-O. Molecular structural differences between low methoxy pectins induced by pectin methyl esterase II: Effects on texture, release and perception of aroma in gels of similar modulus of elasticity. *Food Chemistry*. 2014; 145: 950–955. doi:10.1016/j.foodchem.2013.09.003.
- [29] Funami, T. The Formulation Design of Elderly Special Diets. *Journal of Texture Studies*. 2016;47(4): 313–322. <https://doi.org/10.1111/jtxs.12202>.
- [30] Stuart S, Motz JM. Viscosity in infant dysphagia management: comparison of viscosity of thickened liquids used in assessment and thickened liquids used in treatment. *Dysphagia* 2009; 24(4): 412-422 doi: 10.1007 / s00455-009-9219-y.
- [31] Ong, J. J.-X., Steele, C. M., & Duizer, L. M. Challenges to assumptions regarding oral shear rate during oral processing and swallowing based on sensory testing with thickened liquids. *Food Hydrocolloids*. 2018; 84:173–180. doi:10.1016/j.foodhyd.2018.05.043.
- [32] Garin N, De Pourcq JT, Cardona D, Martín-Venegas R, Gich I, Cardenete J, et al. Cambios en la viscosidad del agua con espesantes por la adición de fármacos altamente prescritos en geriatría. *Nutr Hosp* 2012; 27 (4): 1298-303. DOI:10.3305/nh.2012.27.4.5838.
- [33] Hadde, E. K, Nicholson, T. M, Cichero, J. A. Y. Rheological characterisation of thickened fluids under different temperature, pH and fat contents. *Nutrition & Food Science*., 2015;45(2):270–285. <https://doi.org/10.1108/NFS-06-2014-0053>.
- [34] Cho HM, Yoo W, Yoo B. Steady and dynamic rheological properties of thickened beverages used for dysphagia diets. *Food Sci Biotech* 2012; 21: 1775-9. <https://doi.org/10.1007/s10068-012-0237-4>.
- [35] Quinchia LA, Valencia C, Partal P, Franco MJ, Britode la Fuente E, Gallegos C. Linear and non-linear viscoelasticity of puddings for nutritional management of dysphagia. *Food Hydrocolloids* 2011; 25: 586-93. DOI 10.1016/j.foodhyd.2010.07.006.
- [36] Calleja A, Pintor B, Vidal A, Villar R, Urioste A, Cano I, et al. Características técnicas de los productos alimentarios específicos para el paciente con disfagia. *Nutr Hosp*. 2015; 32 (4): 1401-7 <http://dx.doi.org/10.3305/nh.2015.32.4.9528>.

# Impact of France Nuclear Tests on typhoons and Earthquakes in November 1990

Vladimir Kostin<sup>1\*</sup>, Gennady Belyaev<sup>2</sup>, Olga Ovcharenko<sup>3</sup>, Elena Trushkina<sup>4</sup>

Institute of Terrestrial Magnetism, Ionosphere and Radio Wave Propagation of Russian Academy of Sciences, IZMIRAN, Moscow, Troitsk, Russia

**Abstract**— *The paper investigates the relationship between the development of typhoons and strong earthquakes after the France nuclear tests (NT) in November 1990. It is shown that after the NT acoustic impact on the tropical disturbance of the Pacific Ocean cloud structures self-organized into a system of three interacting category 5 typhoons. The dependence of the earthquakes  $M > 4.6$  and the intensity of these typhoons as well as Typhoon Mike which passed earlier through the Philippine Islands are considered. Areas were found where the impact of typhoons led to earthquakes  $M > 5.4$  of small lithospheric plates.*

**Keywords**— *Pacific, nuclear test, typhoon, earthquake.*

## I. INTRODUCTION

Three mechanisms of interaction between tropical cyclones (TC) and strong earthquakes are usually considered. The first one is that vertical displacements of the Earth's surface in the zones of action of a cyclone and anticyclone can cause a stress release in seismically active regions, as shown by the example of Kamchatka in [1].

The second one is associated with oscillations of long waves excited by TC in the coastal zone. This mechanism has been studied using special seismic sensors at ~ 2800 US stations for more than 10 years [2].

The third one is associated with the lithospheric mechanism of the transfer of the moment of forces from the rarefaction area under the TC when it is located near the edge of the large lithospheric plate adjacent to the small one. This mechanism was considered in the analysis of small lithospheric plate earthquakes with magnitude  $M > 4.5$  without foreshocks of [3].

Note that nonlinear self-organization of internal gravity waves (IGW) in the form of a separate TC or TC chain can occur due to an inhomogeneous geomagnetic field in the presence of a zonal stratospheric wind as shown in the cycle of theoretical papers [4-5]. This situation was observed after a series of American NTs in 1992 [6].

It seems important to return to observations in November 90 after the Nuclear Tests of France in order to understand the features of earthquakes in small lithospheric plates adjacent to the Indo-Australian and Philippine Plates. This paper is devoted to the study of the features of earthquakes in small lithospheric plates adjacent to the Indo-Australian and Philippine Plates. In this regard it seems important to consider in more detail the relationship between TC and strong earthquakes observed in this region after France Nuclear Tests in November 1990.

## II. TYPHOON DEVELOPMENT IN THE EASTERN PACIFIC OCEAN

TC monitoring and forecasting in the Western North Pacific Ocean are in the area of responsibility of the Joint Typhoon Warning Center (JTWC). The results for 1990 are presented in the report [7]. The trajectories and intensity of TC's in November 90 are shown in Fig. 1 according to [7]. Asterisks mark earthquakes  $M > 5.4$  in this region. Intensity - the maximum sustained 1- minute mean surface wind speed, typically within one degree of the center of a tropical cyclone (1 knot = 0.51444 m/s).

Tropical Cyclone 03B was occurred the Bay of Bengal. TC formed on October 31 in the area (7 N 92 E), reached the coast of India on November 3 in the area (18 N 84 E), pick intensity 30 kt, min sea-level pressure (SLP) 1000 mb.

Mike, one of the most intense and destructive Super Typhoon (ST) of 1990, caused havoc in the central Philippine islands, pick intensity - 150 kt, min SLP 885 mb – established 10 Nov 18 UT. Mike downgrade to Tropical Storm (TS) based on interaction with Vietnam coast 16 Nov 12 UT.

Page was the part of the three-storm outbreak which included a pair of TC near the date line: Owen in the northern hemisphere and Sina in the southern hemisphere. Persisting as a discrete disturbance for nearly two weeks before the first warning was issued. 26 Nov 06 UT Page upgrade to TS followed the development of a well defined 75 km diameter eye. Pick intensity 140 kt, min SLP 898 mb.

Owen started as a discrete cloud mass southwest of Hawaii 14-15 Nov. It started to rapidly intensify from tropical depression (TD) to typhoon intensity in less than 18 hours 21-22 Nov. Owen weakened and then reintensified to ST 26 Nov. Pick intensity 140 kt, min SLP 898 mb.

Sina was first noted as a shallow depression within the South Pacific Convergence Zone to the west of Wallis Island. Sina subsequently peaked intensity 230 km/h (124 knot), min SLP 960 hPa during November 26.

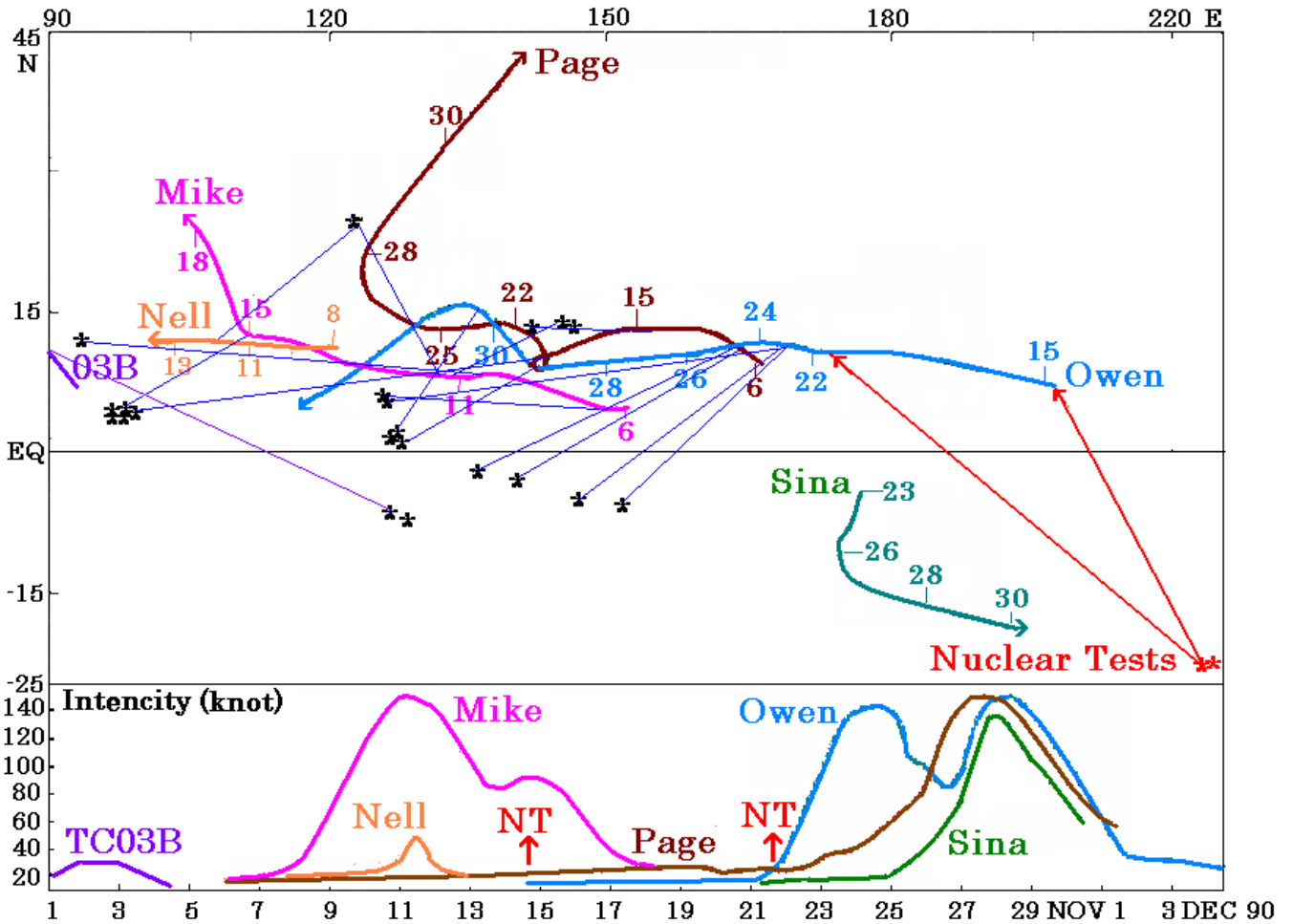


FIGURE 1: Trajectories and intensity of TC. Asterisks mark earthquakes M> 5.4, which are tied to the strongest and nearest TC.

The characteristics of the France underground nuclear test experiments [8] are given in Table 1.

TABLE 1  
NUCLEAR TEST EXPERIMENTS OF FRANCE

No.	Name	Date time UT	Epicenter S / W	Yield kt	Mw
1	Hyrtacos	14 Nov 1990 18:12	22.23 138.34	118	5.5
2	Thoas	21 Nov 1990 17:00	21.85 138.93	36	5.4

### III. LITHOSPHERIC EARTHQUAKES OF INDIA, PHILIPPINES, INDONESIA, NEW GUINEA AND MARIANA ISLANDS

Earthquake data were taken from the United States Geological Survey (USGS) [9]. The region 4 S - 20 N, 92 - 148 E was chosen, 69 earthquakes with a magnitude  $M > 4.6$  were recorded in it in November 1990.

They are concentrated along the main faults of the lithospheric plates. Four areas are highlighted in Tables 2-5 below. Shocks with maximum intensity are highlighted in red and aftershocks are highlighted in blue.

**TABLE 2**  
**EARTHQUAKES OF BIRMA MICRO-PLATE**

No.	Date Nov 90	Area	UT h : m	Epicenter N / E	Mw	Depth km
13	7	coast of northern Sumatra	20:42	5.88 /92.07	4.6	35
19	10	southern Sumatra, Indonesia	11:07	-1.66 /100.48	4.9	80.1
20	10	Andaman Islands, India	11:30	12.21 /93.75	5.4	33
34	15	northern Sumatra, Indonesia	02:34	3.91 /97.46	6.7	48.4
35	15	northern Sumatra, Indonesia	04:48	3.98 /97.32	5.8	30.4
36	15	northern Sumatra, Indonesia	05:18	3.91 /97.29	5.6	53.5
37	15	northern Sumatra, Indonesia	05:47	3.92 /97.35	5.4	48.5
40	16	Simeulue, Indonesia	10:06	2.88 /95.82	4.9	33
42	17	northern Sumatra, Indonesia	02:13	1.26 /99.06	4.9	127.3
44	18	northern Sumatra, Indonesia	16:06	3.88 /97.36	5.1	61.8
45	18	northern Sumatra, Indonesia	16:23	3.94 /97.34	5.5	67.2
51	22	northern Sumatra, Indonesia	17:31	3.81 /95.26	4.8	57.2
57	27	northern Sumatra, Indonesia	00:28	3.22 /98.4	5.1	144.9

The Birma Micro-Plate earthquakes were most strongly impacted by the interaction of Typhoon Mike with the Vietnamese coast on Nov 15-18 and the intensification of Typhoon Owen on Nov 22 and 27 at the edge of the Pacific Plate.

**TABLE 3**  
**EARTHQUAKES OF PHILIPPINE ISLANDS**

No.	Date Nov 90	Area	UT h : m	Epicenter N / E	Mw	Depth km
3	3	Sibuyan Sea, Philippines	15:21	12.9 /122.49	4.7	33
5	4	Molucca Sea	18:26	0.81 /125.19	5.3	33
7	6	Luzon, Philippines	00:37	16.34 /121.1	5.0	10
12	7	Mindanao, Philippines	14:36	5.64 /125.25	5.7	77.8
14	8	Molucca Sea	11:37	2.55 /126.65	4.9	33
22	11	Minahasa, Sulawesi, Indonesia	15:10	0.32 /122.23	5.1	130.9
26	13	Mindanao, Philippines	10:25	9.23 /126.3	4.7	33
38	15	Philippine Islands region	09:43	15.02 /122.04	4.9	22.1
39	15	Molucca Sea	17:32	0.43 /125.32	5.0	33
43	17	Mindanao, Philippines	20:00	5.6 /126.25	4.8	33
46	19	Mindanao, Philippines	01:36	9.89 /126	4.7	124
48	20	Halmahera, Indonesia	09:03	0.17 /127.01	5.8	114.1
50	22	Mindanao, Philippines	05:30	5.02 /125.43	4.9	196.5
52	23	Mindanao, Philippines	07:41	5.54 /125.85	5.5	125
55	25	Philippine Islands region	16:57	10.13 /126.17	4.8	34.5
56	26	Molucca Sea	02:05	1.51 /126.38	4.7	75.4
58	27	Mindanao, Philippines	09:34	7.55 /126.87	4.6	63.5
59	27	Luzon, Philippines	22:49	17.1 /120.09	4.7	65.3
64	29	Mindanao, Philippines	08:02	5.57 /126.78	4.6	217.6
67	30	Minahasa, Sulawesi, Indonesia	13:19	1.03 /123.97	5.8	28.3
68	30	Minahasa, Sulawesi, Indonesia	14:17	1.02 /124.0	5.3	55.3

A very difficult situation was observed in the Philippine Islands in November 90 due to the passage of Typhoons Mike and Owen. However the earthquakes (No. 1-6) were most likely associated with the interaction of TC 03B with the coast of India. The resulting vibrations [2] could be transmitted along the Sunda Trench to the Philippine Plate. The stress release occurred along the Philippine Trench (No. 3 and 5) on 3-4 Nov, in Papua (No. 1) on 1 Nov, on the other side of the Philippine Plate near the Mariana Islands (No. 2, 4, 6) on 2 and 4 Nov.

A crustal earthquake occurred in Luzon at a depth of 10 km on November 6. The remaining 69 earthquakes were lithospheric ones with  $h > 20$  km. This could be due to the fact that tropical disturbance began to develop in the western end of the Pacific Plate in the area (7 N 152 E). If in this case low-frequency oscillations arose, similar to observations [2], then they were captured in the Philippine Trench waveguide and caused a quake (No. 7). Most segments of the Philippines including northern Luzon are part of the Philippine Mobile Belt which geologically and tectonically separate from the Philippine Sea Plate [8]. Seismologists' views on earthquakes of the Philippines can be found for example in article [10].

The cloud system was localized (7.5 N 146 E) and transformed in TD (25 knot) on 7 Nov. as noted by JTWC [7]. A strong earthquake (No. 12) has occurred.

The development of Typhoon Mike was accompanied by separate lithospheric earthquakes at  $h \sim 33$  km on 8-17 Nov.

Deep focus earthquakes occurred at  $h \sim 120$  km on Nov 19-23. Before that in the rarefaction area of Typhoon Mike approaching Vietnam the Sanda Plate was uplifted and, accordingly, was subducting of the Philippine Plate. After the dissipation of Typhoon Mike relaxation occurred along the eastern and southern border of the Philippine Plate - earthquakes (No. 46, 48, 50, 52). The earthquakes are related to the intensification of Owen which passed through the Philippine Plate on 25-30 Nov.

**TABLE 4**  
**EARTHQUAKES OF MARIANA PLATE**

No.	Date Nov 90	Area	UT h : m	Epicenter N / E	Mw	Depth km
2	2	Guam region	11:09	13.78 /143.93	4.8	33
4	4	Northern Mariana Islands	17:57	19.76 /145.32	4.6	171.3
6	4	Guam region	22:23	12.97 /145.2	5.4	51.8
8	6	south of the Mariana Islands	01:54	11.89/143.6	4.8	32.2
9	6	south of the Mariana Islands	10:24	11.83/143.64	4.9	33
10	6	south of the Mariana Islands	14:04	11.87/143.6	4.9	30.8
15	9	south of the Mariana Islands	14:40	11.87 /143.59	4.5	33
16	9	south of the Mariana Islands	15:10	11.92 /143.73	5.0	48.1
17	9	south of the Mariana Islands	23:06	11.83/143.69	4.9	37.9
18	9	south of the Mariana Islands	23:11	11.8 /143.69	4.8	33
21	11	Guam region	11:33	13.84 /144.44	5.4	142.9
24	13	Mariana Islands region	07:15	15.45/147.62	4.8	33
25	13	Mariana Islands region	07:38	15.59/147.8	4.7	33
28	13	Mariana Islands region	12:29	15.57/ 147.81	5.0	31.2
29	13	Mariana Islands region	12:37	15.55/147.73	4.8	33
30	13	Mariana Islands region	22:11	15.64 /147.79	4.7	34.3
32	14	Mariana Islands region	16:30	12.25 /141.14	5.4	126.8
33	14	Mariana Islands region	21:08	15.59 /147.75	4.9	30.2
41	16	Guam region	19:55	12.3 /145	4.5	33
49	21	Mariana Islands region	21:15	15.38 /147.44	4.8	76.4
60	28	Guam region	15:10	13.8 /145.1	4.9	33
62	29	Mariana Islands region	04:29	15.13 /147.48	5.1	31.8
63	29	Mariana Islands region	05:53	15.11 /147.56	4.8	23.3
65	29	Guam region	14:50	13 /143.83	5.1	126.6
66	29	Mariana Islands region	19:12	17.06 /147.24	4.6	69.2
69	30	Northern Mariana Islands	15:24	16.44 /145.74	4.5	543.2

Three quakes (No. 8-10) occurred in an area of ~ 10 km at a distance of 120 km north-east of Challenger Drop on 6 Nov. Typhoon Mike began to form at the western end of the Pacific Plate (7 N 152 E).

Four quakes occurred in the same area (No. 15-18) on 9 Nov. Typhoon Mike intensified to ~ 100 kt and shifted to Caroline Plate (9 N 137 E).

Strong earthquake struck Guam (No. 21) on 11 Nov. Typhoon Mike moved to the southern end of the Philippine Plate (8 N 132 E).

The earthquakes were determined by the movement of Typhoon Mike on 13 - 16 Nov.

Also the earthquakes are associated with the strengthening of Typhoon Owen which passed through the Philippine Plate on 28 - 30 Nov.

**TABLE 5**  
**EARTHQUAKES OF PAPUA AND NEW GUINEA**

No.	Date Nov 90	Area	UT h : m	Epicenter N / E	Mw	Depth km
1	1	Papua, Indonesia	03:39	-3.53 /139.37	5.7	35.3
27	13	coast of Papua, Indonesia	10:30	-2.44 /139.86	5.2	33
31	14	Papua New Guinea	03:14	-3.03 /142.07	5.2	33
47	19	coast of Papua, Indonesia	15:31	-1.77 /134.39	4.9	33
	22	Papua New Guinea	20:49	-5.57 /151	6.3	28.7
	23	Papua New Guinea	00:56	-5.0/145.79	5.7	61.8
53	24	coast of Papua, Indonesia	16:17	-2.03 /135.29	5.3	33
54	24	Papua, Indonesia	18:18	-3.18 /139.55	5.3	36.1
61	28	Papua, Indonesia	19:30	-3.05 /139.53	4.8	33

On 13-14 Nov Earthquakes (No. 27, 31) have struck Woodbark Plate where Caroline Plate and North Bismark Plate abut. Typhoon Mike moved from the Philippine Plate to the area (11 N 122 E) and its impact was transmitted through the Caroline Plate.

On 22-24 Nov after Owen sharp increase a sequence of strong earthquakes due to NT was observed as noted in Fig. 1. Table 5 additionally includes two strongest earthquakes on the South Bismark Plate. The North Bismark Plate separates this plate from the Pacific Plate.

On 28 Nov earthquake (No. 61) struck Woodbark Plate. After Owen crossed the Mariana Trench no earthquakes were recorded in this region until 1 Dec.

#### IV. DISCUSSION OF THE RESULTS

The analysis of the earthquakes data  $M > 2.5$  [9] in the considered area in November 90 showed that in addition to the original list reflected in Tables 2-5 10 lithospheric earthquakes of magnitude 4.3 - 4.5 occurred. Eight earthquakes were in the Mariana Plate, one was at the Birma Plate and one was at Papua. The magnitude of the earthquakes varied from 4.6 to 6.7. The earthquake energy  $E$  in joules will be estimated by the formula (1) which connects it with the magnitude  $M$  [8].

$$M = 2/3(\lg E - 4.8) \quad (1)$$

Then we get that  $E$  varied in the range from 0.501 TJ to 708 TJ (Tera Joule).

Estimation of NT energy (Table 1) according to formula (1) gives in the first case 11.2 TJ and in the second one 7.94 TJ. Calculation of energy through the trotyl equivalent  $Y$  (kt) gives 494 TJ and 151 TJ respectively. This means that in the first case 2.3% of the explosion energy and in the second one 5.3% of it was converted into seismic energy.

The earthquake characteristics indicate that in the cases under consideration the same mechanism of action on the lithospheric plates took place. Let us consider the mechanism in more detail using the example of the South Bismark Plate earthquake on 22 Nov. The initial situation is given in Fig. 2.



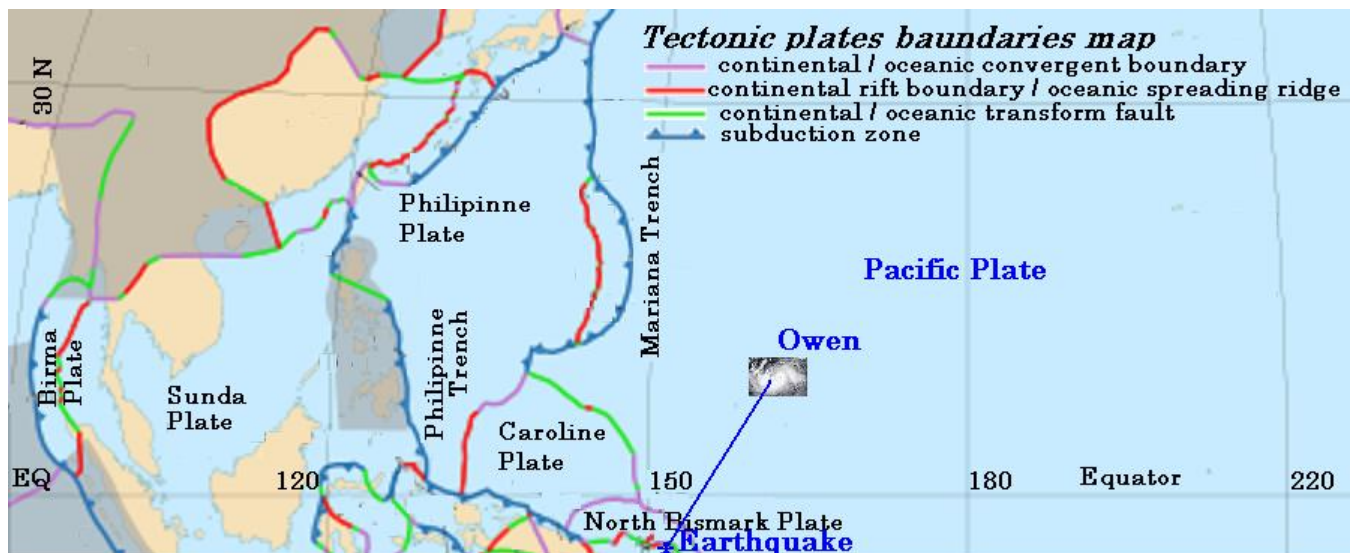


**FIGURE 2: The scheme of interaction between Owen and the earthquake of Earth Bismark Plate 22-Nov-90.**

Owen commenced explosive intensification as a tropical depression experiencing a drop in central pressure of 62 mb in 24 hours [7] one hour after NT Thoas. An eye 35 km in diameter was formed, the diameter of a compact cloud structure ~ 300 km. Let us estimate the force  $F$  lifting the Pacific Plate as the multiplication of the fall pressure on the eye area. This estimate gives  $F = 6 \cdot 10^{12} \text{ N} = 6 \text{ TN}$ .

We consider a large lithospheric plate as a solid, rigid plate interacting with the surrounding plates. In this mechanical system the conservation law of moment of forces is being fulfilled. The ends of the Pacific Plate in this situation will put down and pull the small plates under which it is partially offset. In the most stressed place a rupture occurs part of the small slab breaks off and falls. A new equilibrium is being established.

There are three initial equations, a detailed discussion of which is beyond the scope of this article:

1. The conservation law of moment of forces is written relative to a point on the boundary of the cloud structure for a sector whose angle is equal to the ratio of the transverse length of the collapsed block to the distance between Owen and quake. Longitudinal length is estimated as the distance to an adjacent plate. On the one hand we have the lifting force of the typhoon on the other hand we have the breaking force equal to the multiplication of the ultimate strength by the slab area.
2. Incompressibility of magma. Since the lithospheric plate floats, when it tilts, the volume of displaced magma is equal to the raised one. In the case under consideration the distance between Owen and quake is ~ 1500 km which is less than the Earth's radius and the sphericity is not taken into account. This equation includes the drop height of the slab.
3. The energy released during the South Bismark Plate earthquake is estimated by (1) at 178 TJ and it is equated to the work of the forces of rupture or the potential energy of the collapsed slab.

This physical representation is in good agreement with the numerical parameters of plate tectonics [8]. It explains the lithospheric nature of all earthquakes (Tables 2-5). The depth of most earthquakes is ~ 30 km. In more complex cases of deep lithospheric earthquakes the subsidence of the large lithospheric plate must of course be taken into account.

It should be noted that three out of four NTs in the US in June and September 1992 affected TC [6]. The TCs changed their intensity and movement direction. The 7.2-magnitude crustal earthquake Landers 92 occurred when Hurricane Selia reached its maximum. The earthquake mechanism is in good agreement with the concepts of [2].

Analysis of the strongest earthquakes in California over the past 30 years has shown that they can be associated with the development of TC [6]. Moreover the earthquakes east of the San Andreas Fault had foreshocks. An algorithm for analyzing foreshocks is proposed, it gives the place and approximate time of the main quake. Earthquakes west of the San Andreas Fault have no foreshocks. The presentation of the report in Russian 22 pages is attached to the theses [6], which can be opened by clicking on the appropriate index.

Forecasting the development of seismic activity for a number of different geophysical parameters of the environment both on the ground and from satellites is of great practical importance [12].

A preliminary analysis of seismic activity in November 1990 showed that it intensified after strengthening of TC Sina under the influence of NT Thoas on the American continent.

## V. CONCLUSION

1. Almost all lithospheric earthquakes in the regions adjacent to the Philippine Plate can be explained in terms of the impact of tropical cyclones in November 90.
2. France Nuclear Tests acoustic impact on tropical disturbance areas led to their self-organization to the intensity of super typhoons in November 90.
3. Preliminary analysis showed that the TC impact on the Pacific Plate in November 90 was transferred to the area of Mid-American Trench and Peru-Chile Trench. A detailed analysis of these events will be presented.

## ACKNOWLEDGEMENTS

Cosmos-1809 monitored NT from 1987 to 1992 on the instructions of the Seismic Control Service (scientific supervisor academician V.V. Migulin [11]). The authors would like to thank the project participants for their joint research on the NT impact on the environment.

The authors are grateful to director of IZMIRAN V.D. Kuznetsov for support of the work.

The writing of this work was supported by Kaskad LLC, Moscow, General Director E.S. Golubov.

## REFERENCES

- [1] V.N. Bokov, and V.N. Vorobyev, "Atmospheric processes initiating the focal mechanism of earthquakes," Scientific notes of RGGMU, vol. 51, pp. 9-21, 2018.
- [2] W. Fan, J. J. McGuire, C. D. de Groot-Hedlin, M. A. H. Hedlin, S. Coats, and J. W. Fiedler, "Stormquakes," Geoph. Research Letters, vol. 46(22), pp. 12909-12918, doi: 10.1029/2019GL0842217, 2019.
- [3] V. Kostin, G. Belyaev, O. Ovcharenko, and E. Trushkina, "Features of some interacting tropical cyclones in the Indian Ocean after the Mount Pinatubo eruption," Intern. J. Engineering Research & Science, vol. 5(9), pp. 19-26, doi: 10.5281/zenodo.3465257, 2019.
- [4] G.D. Aburjania, "Self-localization of planetary wave structures in the ionosphere upon interaction with nonuniform geomagnetic field and zonal wind," Izvestiya, Atmospheric and Oceanic Physics, vol. 47 (4), pp. 533-546, 2011.
- [5] G.D. Aburjania, O.A. Kharshiladze, and K.Z. Chargazia, "Self-organization of IGW structures in an inhomogeneous ionosphere: 2. Nonlinear vortex structures," Geomgn. Aeron., vol. 53 (6), pp. 750-760, doi: 10.1134/S0016793213060029, 2013.
- [6] V.M. Kostin, G.G. Belyaev, O.Ya. Ovcharenko, and E.P. Trushkina, "The relationship between the development of tropical cyclones and strong earthquakes in June 1992 according to the monitoring of the plasma of the ionosphere from the satellite Cosmos-1809," Proceeding of the 18<sup>th</sup> conference "Modern problems of remote sensing of the Earth from space", pp. 401+22, doi: 10.21046/18DZZconf-2020a, 2020, <http://conf.rse.geosmis.ru>.
- [7] D.K. Rudolph, and C.P. Guard, "Annual tropical cyclone report," Joint typhoon warning center, Guam, Mariana island, 279 p. 1990.
- [8] <https://www.wikipedia.org>.
- [9] <https://earthquake.usgs.gov/earthquakes/search>.
- [10] Wen-Nan Wu, Chung-Liang Lo, and Jing-Yi Lin, "Spatial variations of the crustal stress field in the Philippine region from inversion of earthquake focal mechanisms and their tectonic implications," J. Asian Earth Sciences, vol. 142 (7), pp. 109-118, doi: 10.1016/j.jseaes.2017.01.036, 2017.
- [11] V.M. Kostin, and V.D. Murashev, "Experimental studies of the possibilities of satellite radio monitoring of underground nuclear tests," in Born of the atomic age, vol. III, A.P. Vasil'ev, Eds. Moscow, 2002, pp. 178-191.
- [12] S.A. Pulinets, D.V. Davidenko, D.P. Ouzounov, and A.V. Karelin, "Physical bases of the generation of short-term earthquake precursors: A complex model of ionization-induced geophysical processes in the lithosphere-atmosphere-ionosphere-magnetosphere system," Geomagn. Aeron., vol. 55(4), pp. 521-538, doi: 10.1134/S0016793215040131, 2015.



**AD Publications**

**Sector-3, MP Nagar, Bikaner,  
Rajasthan, India**

**[www.adpublications.org](http://www.adpublications.org), [info@adpublications.org](mailto:info@adpublications.org)**